ESAIM: M2AN 42 (2008) 507–533
DOI: 10.1051/m2an:2008015

ESAIM: Mathematical Modelling and Numerical Analysis
www.esaim-m2an.org

OPTIMAL POISEUILLE FLOW IN A FINITE ELASTIC DYADIC TREE

Benjamin Mauroy[1] and Nicolas Meunier[2]

Abstract. In this paper we construct a model to describe some aspects of the deformation of the central region of the human lung considered as a continuous elastically deformable medium. To achieve this purpose, we study the interaction between the pipes composing the tree and the fluid that goes through it. We use a stationary model to determine the deformed radius of each branch. Then, we solve a constrained minimization problem, so as to minimize the viscous (dissipated) energy in the tree. The key feature of our approach is the use of a fixed point theorem in order to find the optimal flow associated to a deformed tree. We also give some numerical results with interesting consequences on human lung deformation during expiration, particularly concerning the localization of the *equal pressure point* (EPP).

Mathematics Subject Classification. 74D05, 74Q10, 76S05, 92B05.

Received December 22, 2006. Revised September 27, 2007.
Published online May 27, 2008.

1. Introduction

The goal of this paper is to study mathematically and numerically the interaction between a finite dyadic elastic tree made of cylindrical pipes and the fluid that goes through it. The fluid is assumed to be viscous, to have given fluxes at the outlets and to flow according to Poiseuille's law. First we consider the case of a rigid tree. Following [3], we establish a relationship between the fluxes and the pressures at the leaves in the case of a non regular tree (*i.e.* a regular tree has constant radii at each generation). However, in the contrary of [3] where the tree considered is rigid, we assume that the tree branches have elastic walls. Under the assumptions that the elastic deformation's law of the pipes is linear and that the pipes stay cylindrical after deformation, we give a stationary model of the branch deformation mechanism. The deformed radius of each branch is obtained by considering the balance between the internal pressure due to the fluid flow and the external pressure due to some strains. Although, the pipe's elastic law and the relation between the pressure and the flux are linear, the elastic model of the branch deformation mechanism is nonlinear and the main difficulty of this problem stays in the geometry of the tree. Then, considering a viscous energy term, we study an optimization problem for fluxes at the outlets with respect to a tree. Generally, the given fluxes and the deformed tree do not satisfy this optimality condition, that is to say that the dissipated energy of the flow in the deformed tree has not

Keywords and phrases. Fixed point, Poiseuille flow, finite tree, elastic wall, lungs, equal pressure point.

[1] Laboratoire MSC, Université Paris 7 (Denis Diderot), 2 place Jussieu, building 33/34, 75251 Paris Cedex 05, France.
benjamin.mauroy@paris7.jussieu.fr

[2] Laboratoire de Mathématiques MAP5, Université Paris 5 (R. Descartes), 45 rue des Saints Pères, 75006 Paris, France.
Nicolas.Meunier@math-info.univ-paris5.fr

Article published by EDP Sciences

a minimal value. In order to find a more realistic deformed tree in the sense that the dissipated energy of the flow in the deformed tree has an optimal value, we use a fixed point theorem.

A motivation for this modeling problem is the construction of a simple and global mechanical model of the central region of the human lung in the case of small deformations. The bronchial tree of the human lung can be viewed as a dyadic net of pipes composed of 23 generations. More precisely, according to [5–7,12], we can distinguish three parts in this tree. In the first part, mainly from the first generation to the fifth generation, there is some cartilage and the pipes can be assumed to be rigid. Moreover, the effects of inertia in the flow are large and correspond to the nonlinear Navier-Stokes regime. In the middle part, mainly from the sixth generation to the sixteenth generation, the effects of inertia are smaller. This validates the Poiseuille regime (see [3,5–7,12]), at least for rest respiratory regime. In this part of the tree, cartilage does not exist and there are interactions between the fluid and the walls of the pipes. In the last part, the tree function becomes different (beginning of gas exchange with blood).

The plan of the paper is as follows. We begin with some notations in Section 2. Assuming that some incompressible, viscous and non-inertial fluid flows through a single pipe, our first step, in Section 3, consists in modeling the deformation mechanism of the pipe. Then, in Section 4, we consider a finite dyadic tree and we express the deformation for the whole tree when air flows through it according to Poiseuille's law. In Section 4, we build the optimal air flow distribution at the leaves of the tree that minimizes an energy functional corresponding to the dissipated viscous energy for a given tree. In Section 5, using a fixed point theorem, we prove the existence of a deformation and of an air flow distribution such that this air flow applied to the tree minimizes the energy functional associated to this tree after deformation. Finally, in Section 6, we present a few numerical simulations and applications of this theory to the human lung, particularly concerning the localization and progression of the *equal pressure point* (EPP). This point is defined as the point (indeed the pipe in our case) of the tree where the deformation is equal to zero and which is such that before this point, there is an inflation and after this point there is a reduction of the radii. In Appendix, we give the details about the numerical scheme used to compute the fixed point defined in Section 5 and we give some estimates to determine the convergence condition and convergence speed of the scheme.

2. Notations

Let us begin with a short review of the different notations that will be used.

The set of square real matrices (resp. invertible real matrices, symmetric real matrices and symmetric positive definite real matrices) of size $N \times N$ is denoted $\mathcal{M}_N(\mathbf{R})$ (resp. $GL_N(\mathbf{R})$, $S_N(\mathbf{R})$ and $S_N^{+*}(\mathbf{R})$). Some other matrix sets will be introduced in Section 4 and Appendixes A and B (such as $\mathcal{B}_N$ and $\mathcal{P}_N$). We will use the matrix norm $|||.|||_2$ subordinate to the Euclidean norm $||.||_2$ (*i.e.* if $M = (m_{ij})$ then $|||M|||_2 = \sup_{X \neq 0} \frac{||MX||_2}{||X||_2}$).

A vector $(a_0, a_1, ..., a_N)$ will be such that a_i is at position i.

A tree of height N will be denoted by $\mathcal{T}_N$, the nodes and branches will be indexed by i and the generation number will be denoted by $k(i)$. The notion of path Π on the tree will be introduced in Section 4. The total outgoing flux in the root node will be denoted by Φ, while $\mathbf{q}_{\mathcal{T}_N}$ (resp. $\mathbf{p}_{\mathcal{T}_N}$) will denote the vector whose components (denoted by $\tilde{p}_i$ (resp. $\tilde{q}_i$)) are the fluxes (resp. the pressures) in the branches (resp. at the nodes) and $\mathbf{q}$ (resp. $\mathbf{p}$) will denote the vector whose components (denoted by p_i (resp. q_i)) are the fluxes (resp. the pressures) at the outlets. Several exterior pressure values P_{ext}, P_{ext}^1 and P_{ext}^2 will be introduced in order to allow to solve equation from which the radius $\mathbf{r}$ of the deformed tree will be deduced (our approach is stationary).

The symbol J will denote the real vector made of ones, *i.e.* $J = {}^t(1, ..., 1)$. Its size will correspond to the number of leaves of the tree $\mathcal{T}_N$ considered, namely 2^N.

Cylindrical coordinates (x, θ, z) will be used.

The symbol $\sim$ will be used for equivalent functions.

3. Branch deformation mechanism

In this section, we present the deformation mechanism in the case of a single branch B. The deformation mechanism for the whole tree will be presented in Section 4. We consider an incompressible, viscous and non-inertial fluid which flows through a single elastic pipe and we look for the deformed pipe.

First, for such a fluid, we recall that the pipe is characterized by its resistance which is the ratio of the pressure jump between its ends over the flux. Next, assuming that the branch stays cylindrical after deformation and that the constitutive law of the wall is linear, we build an elastic model of the branch deformation mechanism (which is nonlinear because hydrodynamical resistance is a nonlinear function of branch radius) depending on the pressure jump between the inside and the outside of the branch.

In the case of the human lung, the assumption that the pipe remains cylindrical can be explained as follows. First, the variation of the external (and internal) pressure in the pipe is small and can be assumed to be equal to zero. Next, for those pipes located between the 6th and the 16th generations, there exists an external strain which acts on all pipes through smooth muscles (with spiral shapes along the pipe wall).

Let us begin with some notations used in this section. B is a cylindrical elastic pipe of radius r and of length L. The pressure is supposed to be uniform over each end section. The inlet is referred to a (for above) and the outlet to b (for below). The flow q going through B is chosen positive when the fluid goes from b to a. We assume that the branch is submitted to a uniform external pressure P_{ext}.

3.1. The Poiseuille law

Here, we assume that the pipe is rigid so that there is no interaction between the fluid and the pipe. In such a case, the external forces acting on the fluid can be characterized by both values P_a and P_b. The linearity of the Stokes equations ensure the existence of a coefficient $R > 0$ which relates the flux q and the pressure jump $P_a - P_b$

$$P_a - P_b = Rq. \tag{3.1}$$

By analogy with electric conductors (flux and pressure respectively play roles of intensity and potential), R is called the resistance of the pipe. It depends on the geometrical characteristics of the pipe and on the viscosity μ of the fluid:

$$R = \frac{8\mu L}{\pi r^4} = C\frac{L}{r^4}, \quad C > 0. \tag{3.2}$$

3.2. Flow through an elastic pipe

Now we consider interactions between the fluid and the pipe. Let $r(z)$ denote the equilibrium radius of a section of the branch. It depends on the position z on the axis $[0, L]$. Under the following hypothesis:

(1) the pipe remains cylindrical after deformation, *i.e.* $r(z) = r$;
(2) the fluid flow is stationary (fluid pressure and velocity are not time-dependent);

we first prove that the equilibrium state of the branch is such that its radius is a positive root (if it exists) of the equation:

$$-t(r)r^3 + (P_a - P_{ext})r^4 + \frac{CqL}{2} = 0, \tag{3.3}$$

where t is the superficial lineic tension and P_{ext} is the external pressure. Since our approach is stationary, we give mechanical data corresponding to different states of the branch. These data will allow to solve (3.3). We end this section by solving (3.3) and by giving bounds on the solution which will be useful for the constrained minimization problem (fixed point theorem).

3.2.1. *Equilibrium state of the branch*

Let us establish (3.3). To do so, consider a small portion of a branch δB (see Fig. 1). The superficial lineic tension is given by a function t which depends on the radius r of the branch. In order to force the branch to stay

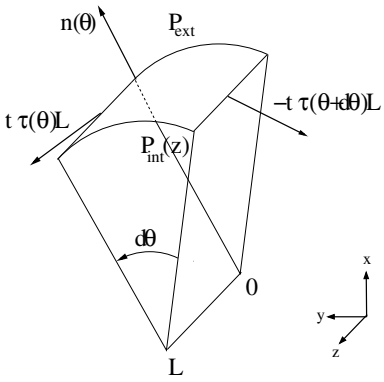

FIGURE 1. Tangential forces orientations on an element $\mathrm{d}S$ of the branch surface.

cylindrical, we introduce the following tangential force F_t. It is tangent to the branch surface and the resulting force on δB is:

$$\mathrm{d}F_t = t(r)\tau(\theta)L - t(r)\tau(\theta + \mathrm{d}\theta)L,$$

where τ is the tangential vector.

The external pressure force on a small area $\mathrm{d}S = r\,\mathrm{d}\theta\,\mathrm{d}z$ is given by the external pressure times the surface, *i.e.* $P_{ext}\,\mathrm{d}S$. Its direction is normal to the surface (along vector $n(\theta)$) and inward the center of the branch. Since the external pressure is assumed to be constant all around the pipe, on δB, we have:

$$\mathrm{d}F_{P_{ext}} = -\int_0^L \int_\theta^{\theta+\mathrm{d}\theta} P_{ext} n(\eta) r\,\mathrm{d}\eta\,\mathrm{d}z = -P_{ext} rL \int_\theta^{\theta+\mathrm{d}\theta} n(\eta)\,\mathrm{d}\eta.$$

The internal pressure $P_{int}(z)$ at position $z \in [0, L]$ is due to the flow q inside the branch and is given by Poiseuille relation (3.1) with (3.2):

$$P_{int}(z) = P_a + C\frac{z}{r^4}q.$$

Hence the mean internal pressure P_{int} in the branch is

$$P_{int} = P_a + C\frac{L}{2r^4}q.$$

Since we assume that the pipe stays cylindrical after deformation (which can be viewed as saying that the internal pressure is supposed to be constant and equal to its mean value thanks to the fact that the external pressure is constant), the internal mean pressure forces acting on the portion of branch is directed along $n(\theta)$ and from the center of the branch toward its surface and is given by:

$$P_{mean} = rL\,\mathrm{d}F_{P_{int}},$$

with

$$\mathrm{d}F_{P_{int}} = \left(P_a rL + \frac{Cq}{r^3}\frac{L^2}{2}\right)\int_\theta^{\theta+\mathrm{d}\theta} n(\eta)\,\mathrm{d}\eta.$$

Moreover, we have:

$$\int_\theta^{\theta+\mathrm{d}\theta} n(\eta)\,\mathrm{d}\eta = -\tau(\theta + \mathrm{d}\theta) + \tau(\theta) = n(\theta)\,\mathrm{d}\theta.$$

Hence, if δB is at equilibrium:

$$0 = \mathrm{d}F_t + \mathrm{d}F_{P_{ext}} + \mathrm{d}F_{P_{int}} = \left[t(r)L + (P_a - P_{ext})rL + \frac{CqL^2}{2r^3}\right] n(\theta),$$

therefore, the equilibrium state of the branch is such that its radius is a positive root (if it exists) of (3.3).

3.2.2. *Mechanical data and definitions*

Let us now give some mechanical data on the branch which describe its mechanical behavior. This will allow us to solve equation (3.3). First, in the sequel P_0 will denote a fixed pressure value.

More precisely, we will define three specific branch radii corresponding to different values of pressure and flux appearing through this model. The different radii of a branch B are linked together through mechanical equilibrium equations. Let us briefly explain how it works. The branch is assumed to have an unconstrained radius r^0 under the pressure P_0 (see (3.6) below). For human lung, this state will correspond to the case of a dead body. The lung is almost collapsed. Then, we modify the exterior pressure to P^1_{ext} and we consider that there is no flow inside the branch. The radius of the pipe is r^e solution of (3.7) (see below). This radius r^e corresponds to Weibel's data [12] and r^0 is calculated from r^e equilibrium equation (3.7). We assume that

$$P^1_{ext} \neq P_0. \tag{3.4}$$

The last step consists in modifying the exterior pressure to P^2_{ext} and in applying a non-negative flux q through the pipe. Hence, we obtain the final radius r. Since we consider expiration, we assume that

$$P^2_{ext} > P^1_{ext}. \tag{3.5}$$

Let us now go further into details.

Definition 3.1. *Unconstrained radius:*
We denote by r^0 the branch radius satisfying

$$t(r^0) = 0. \tag{3.6}$$

It is a solution of (3.3) when $P_{ext} = P_a = P_0$ and when there is no flow going through the branch, *i.e.* $q = 0$.

Definition 3.2. *Initial radius:*
We denote by r^e the radius which corresponds to the branch geometry (*i.e.* solution of (3.3)) when $P_{ext} = P^1_{ext}$ satisfying (3.4), $P_a = P_0$ and when there is no flow inside the branch. In this case, this geometry r^e satisfies the following equilibrium:

$$-t(r^e) + (P_0 - P^1_{ext})r^e = 0. \tag{3.7}$$

In the sequel, it will be referred to as an *initial state*.

Definition 3.3. *Final radius:*
We denote by r a solution of equation (3.3), if it exists, when $P_{ext} = P^2_{ext}$ with (3.5) and the flux q is given, assumed to be non-negative. This situation corresponds to a deformed branch with a flow q inside. It will be referred to as a *final state*.

Let us now explain the elastic law t, we consider the linear case:

$$t(r) = \tilde{E}(w)\left(\frac{r}{r^0} - 1\right),$$

where $\tilde{E}(w)$ depends on the Young modulus and the width w of the branch. More precisely, the term $\tilde{E}(w)$ is a lineic force and corresponds to the resultant of elasticity forces on a unit section of bronchial wall, hence this corresponds to Ew where E is the Young modulus, see Figure 2.

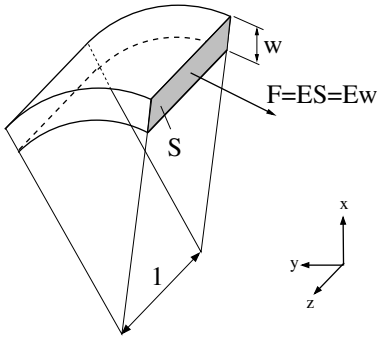

FIGURE 2. The lineic elastic force $\tilde{E}(w)$ acting on the gray section S can be written $F = ES = E \times w \times 1$, where E is the material Young modulus and w its thickness, F units are N/m. Hence $\tilde{E}(w) = Ew$.

Note that such a definition corresponds to a one-dimensional string model for walls behavior. In particular, it neglects the wall deformations in other directions than the longitudinal one (like thickness changes). This choice is a coherent approximation with the preceding approximations of small deformations and constant radius along the whole branch. Note that it also limits the number of parameters involved in the model. It is however possible to give an alternate definition assuming thin plate behavior and involving the Poisson's ratio ν of the branch walls. In this case, $\tilde{E}(w)$ could be expressed by $Ew/(1-\nu^2)$. Because tissues are almost incompressible, $\nu \sim 1/2$ and this induces a supplementary $4/3$ factor to our choice of $\tilde{E}(w)$.

According to data from [10], we use a linear dependence between bronchial radius and bronchial wall thickness of the type: $w = \gamma r^e$. In [10], estimated values of γ are between $2/5$ and $1/2$. In the following we will use $\gamma = 2/5$, hence

$$t(r) = \frac{2}{5} E r^e \left(\frac{r}{r^0} - 1 \right). \tag{3.8}$$

Although such a law is not realistic in the sense that $t(r)$ does not tend to $-\infty$ when r goes to zero (which should be the case in order to describe the fact that the branch cannot collapse *in vivo*), it is a good approximation for a first study.

Remark 3.4. The existence of r^e depends on the sign of $P_0 - P^1_{ext} + \frac{2E}{5}$, which we assume from now on to be positive. Moreover, we assume that $r^e \geq r^0$, which corresponds to

$$P_0 \geq P^1_{ext}. \tag{3.9}$$

3.2.3. *Study of equation* (3.3) *and definition of* $q \to r(q)$*:*

In this paragraph, we study hypothesis under which equation (3.3) admits a unique solution, we give some monotonicity results and we state some estimates on the radii and pressures. These properties are necessary in order to obtain the existence of a deformed tree, see below Section 4. This part is rather technical and it can be left apart by the reader who is interested in the modelling part of this work.

More precisely, we assume that (3.5)–(3.9) are satisfied and that the inlet pressure satisfies $P_a \in]P_a^{min}; P_a^{max}[$ with P_a^{min}, P_a^{max} given. Let $r^0 > 0$ and $r^e > 0$ satisfy (3.6) and (3.7) respectively with $t(r)$ given by (3.8) and

$$L = 6r^e. \tag{3.10}$$

This last hypothesis corresponds to physiological observations which show that in average length over radius of the branches of the lung is close to six [12,13].

Recalling (3.7) and (3.8), equation (3.3) becomes:

$$-\frac{\frac{2E}{5}+(P_0-P_a)+(P^2_{ext}-P^1_{ext})}{\frac{2Er^e}{5}}r+1+\frac{15Cq}{2Er^3}=0, \tag{3.11}$$

which, for simplicity, we rewrite as:

$$g_\alpha(r,q)=\alpha\frac{r}{r^e}+1+\eta\frac{q}{r^3}, \tag{3.12}$$

with

$$\alpha=-1-\frac{5\Big((P_0-P_a)+(P^2_{ext}-P^1_{ext})\Big)}{2E} \text{ and } \eta=\frac{15C}{2E}>0. \tag{3.13}$$

Proposition 3.5. *Let $q\geq 0$ and $\alpha<0$ be fixed, then $g_\alpha(r,q)=0$, with $g_\alpha(r,q)$ given by (3.12), admits a unique solution that is denoted by $r^\alpha(q)$. Moreover, $\alpha\to r^\alpha(q)$ and $q\to r^\alpha(q)$ are increasing functions. Furthermore, the function $q\to r^\alpha(q)$ is C^∞.*

Proof. Let $q\geq 0$ and $\alpha<0$ be fixed. Using the continuity and the strictly decreasing character of the function $r\to g_\alpha(r,q)$ on $]0,+\infty[$ together with $\lim_{r\to 0^+} g_\alpha(r,q)=+\infty$ if $q>0$ or $\lim_{r\to 0^+} g_\alpha(r,q)=1$ if $q=0$ and $\lim_{r\to+\infty} g_\alpha(r,q)=-\infty$, we obtain the existence and uniqueness of the root $r^\alpha>0$.

Let $\alpha_1<\alpha_2<0$, by definition, $g_{\alpha_1}(r^{\alpha_1},q)=g_{\alpha_2}(r^{\alpha_2},q)=0$ and $g_{\alpha_2}(r^{\alpha_1},q)=(\alpha_2-\alpha_1)\frac{r^{\alpha_1}}{r^e}>0$, then we deduce the increasing character $\alpha\to r^\alpha(q)$ from the decreasing character of $r\to g_\alpha(r,q)$.

The increasing character of $q\to r^\alpha(q)$ is obtained similarly. □

Proposition 3.6. *Under the same hypothesis as Proposition 3.5, the function $r_e\to r^\alpha(q)$ is increasing and*

$$r^\alpha(q)\overset{r_e\to 0^+}{\sim}\left(-\frac{\eta q r_e}{\alpha}\right)^{\frac{1}{4}} \quad \text{and} \quad r^\alpha(q)\overset{r_e\to+\infty}{\sim}-\frac{r_e}{\alpha}.$$

Proof. The increasing property is shown similarly as in the previous proposition and the equivalents are a direct consequence of the definition of g_α. □

Remark 3.7. In this remark we give some estimates which will be used for the recursive construction of the deformed tree (see Sect. 4).

Assume that there exists $q^{max}>0$ and $\alpha^{min}\leq\alpha^{max}<0$, with $q\in[0;q^{max}]$ and $\alpha\in]\alpha^{min};\alpha^{max}[$. From Proposition 3.5, we deduce that $0<r^{\alpha^{min}}(q^{min})\leq r^\alpha(q)\leq r^{\alpha^{max}}(q^{max})$. In the sequel, we will simply denote $r^{\alpha^{min}}(q^{min})$ by r^{min} and $r^{\alpha^{max}}(q^{max})$ by r^{max}.

The existence of $\alpha^{max}<0$ is satisfied when

$$P_a^{max}<P_0+(P^2_{ext}-P^1_{ext})+\frac{2E}{5}, \tag{3.14}$$

which corresponds to a value for P^2_{ext} and/or to values for E that are large enough.

Moreover, we have that $P_b^{min}\leq P_b\leq P_b^{max}$, with $P_b^{min}=P_a+6C\frac{r^e}{\left(r^{max}\right)^4}q^{min}$ and $P_b^{max}=P_a+6C\frac{r^e}{\left(r^{min}\right)^4}q^{max}$.

4. Finite tree

We start this section with some notations and definitions for finite tree. Then for a rigid tree we state the relations between the fluxes at the leaves and the pressures in the nodes. In such a case, there is no interaction between the fluid and the tree. The main difference with [3] is that we study more general rigid trees (non regular trees) for which the branch radii are non constant on a same generation. This study, which is technical, is needed in order to construct the deformed tree in the general case. Then, we consider the case of an elastic tree and we investigate the deformation mechanism described in the previous section for the elastic pipes (composing

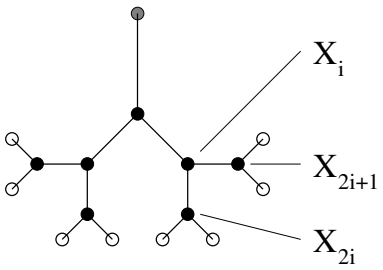

FIGURE 3. A four generation tree scheme ($N = 3$): the nodes are represented by the disks (total number $2^{N+1} = 16$), while the branches are represented by lines (number $2^{N+1} - 1 = 15$). The root node is the gray filled disk, the $2^N = 8$ leaf exits are the blank disks.

the tree) in which an incompressible, viscous, non-inertial fluid flows. Note that a more theoretical study of finite and infinite tree was done in [8].

4.1. Notations and preliminaries

From now on, we will consider a finite dyadic three dimensional tree with $N + 1$ generations (of height N). It will be denoted by $\mathcal{T}_N$. In such a tree, there are the root, 2^N leaves, 2^{N+1} nodes and $2^{N+1} - 1$ branches. We denote by $\mathcal{X}_N = \{X_0, (X_i)_{1\leq i\leq 2^{N+1}-1}\}$ the set of the nodes, where nodes are indexed by 0 for the root node and $i \in \{1, ..., 2^{N+1} - 1\}$ for the other nodes. We use the convention that the two nodes steaming from X_i are X_{2i} and X_{2i+1}, see Figure 3. The set of branches is $\mathcal{B}_N = \{(B_i)_{1\leq i\leq 2^{N+1}-1}\}$ with the convention that branch i ends at node i.

Definition 4.1. Let k and l be the mappings defined as follows:

$$\begin{aligned} k &: i \in \mathbf{N}^* \to k(i) \in \mathbf{N} \text{ such that } 2^{k(i)} \leq i \text{ and } 2^{k(i)+1} > i, \\ l &: i \in \mathbf{N}^* \to l(i) = i - 2^{k(i)}. \end{aligned}$$

If i is a branch or a node index, then $k(i) \in \{0, ..., N\}$ indicates the generation number and $l(i) \in \{0, ..., 2^k - 1\}$ is the position on the k-th generation.

For simplicity, when i is given, we denote $k(i)$ and $l(i)$ by k and l.

Definition 4.2. A tree is said to be *regular* if the radii (resistances) have a constant value on each generation.

In order to establish a relationship between the fluxes at the leaves and the pressures at the leaves in the case of a non regular tree (see Prop. 4.6 below), we have to "follow" the fluid through paths in the tree. Therefore, it is necessary to define the notions of path and sub-path on $\mathcal{T}_N$.

Definition 4.3. Let $i \in \{1, ..., 2^{N+1} - 1\}$ be given, the set of the indices of branches corresponding to the $k(i) + 1$ branches that link the root node to the i-th node is denoted by $\Pi_{0\to i}$. It is the set of strictly increasing integers:

$$\Pi_{0\to i} = \left\{ \left[\frac{i}{2^k}\right] = 1, ..., \left[\frac{i}{2}\right], i \right\}, \tag{4.1}$$

where [.] denotes the integer part.

Let $m \in \{0, ..., k(i)\}$, $\Pi_{0\to i}(m)$ is the subset of $\Pi_{0\to i}$ defined by

$$\Pi_{0\to i}(m) = \left\{ \left[\frac{i}{2^{k(i)}}\right] = 1, ..., \left[\frac{i}{2^{k(i)-m}}\right] \right\}. \tag{4.2}$$

4.2. **Flow through a rigid dyadic tree**

We consider an incompressible, viscous and non-inertial fluid which flows through a tree $\mathcal{T}_N$ of connected pipes. Each pipe is characterized by its resistance see (3.1) and (3.2). Our first step, as in [3], consists in establishing a relationship between pressures and fluxes at the leaves.

4.2.1. *Pressure, flux, resistance and radius associated with* $\mathcal{T}_N$

In the sequel, we will denote by P_{root} the pressure at the root node that we will assume to be non-negative. We will denote by P_0 a reference pressure that we will also assume to be non-negative. Practically, P_0 will correspond to atmospheric pressure. Moreover, in the case of the human lung, the region where this analysis could be valid is the central region, hence the pressures P_0 and P_{root} are different. Furthermore, since we study the expiration phase, we assume that

$$P_{root} > P_0. \tag{4.3}$$

We denote by $\mathbf{p}_{\mathcal{T}_N}$ (resp. $\mathbf{q}_{\mathcal{T}_N}$, $\mathbf{r}_{\mathcal{T}_N}$ and $\mathcal{R}_{\mathcal{T}_N}$) the pressure vector (resp. flux, radius and resistance vectors) whose components are the pressure (resp. flux, radius and resistance) on the nodes (resp. branches) of $\mathcal{T}_N$. Since the pressure at the root node is given by P_{root}, this can be written as:

$$\mathbf{p}_{\mathcal{T}_N} = {}^t(P_{root}, \tilde{p}_1, \tilde{p}_2, ..., \tilde{p}_{2^{N+1}-1}) \text{ and } \mathbf{q}_{\mathcal{T}_N} = {}^t(\tilde{q}_1, \tilde{q}_2, ..., \tilde{q}_{2^{N+1}-1}).$$

The vectors $\mathbf{r}_{\mathcal{T}_N}$ and $\mathcal{R}_{\mathcal{T}_N}$ are defined similarly to $\mathbf{q}_{\mathcal{T}_N}$. Furthermore, the total resistance associated with the path $\Pi_{0\to i}$ is:

$$\mathcal{R}_{\Pi_{0\to i}} = \sum_{j\in\Pi_{0\to i}} \tilde{R}_j.$$

For the radius and the resistance associated with a tree, we will omit the subscript, when no confusion arises.

4.2.2. *Relation between pressure and flux at leaf exits of* $\mathcal{T}_N$

From now on, leaf exits of the tree will be indexed by $0, ..., 2^N - 1$. Moreover, the pressure (resp. flux) vector at leaf exits will simply be denoted by $\mathbf{p}$ (resp. $\mathbf{q}$) with:

$$\mathbf{p} = {}^t(p_0, ..., p_{2^N-1}) \quad \text{and} \quad \mathbf{q} = {}^t(q_0, ..., q_{2^N-1}).$$

Remark 4.4. Recalling notations introduced in the previous section we have

$$\mathbf{p} = {}^t(\tilde{p}_{2^N}, ..., \tilde{p}_{2^{N+1}-1}) \quad \text{and} \quad \mathbf{q} = {}^t(\tilde{q}_{2^N}, ..., \tilde{q}_{2^{N+1}-1}).$$

Definition 4.5. Given two positive integers i and j and their binary expansions

$$i = \sum_{k=0}^{\infty} \alpha_k 2^k, \ j = \sum_{k=0}^{\infty} \beta_k 2^k, \text{ with } \alpha_k, \beta_k \in \{0, 1\}, \ \forall k,$$

we define $\nu_{i,j}$ as

$$\nu_{i,j} = \inf\{k \geq 0, \ \alpha_l = \beta_l, \ \forall l \geq k\}. \tag{4.4}$$

Let us now state the relation between pressure and flux at leaf exits. Since the proof is similar to the one which was done in [3] (Prop. 1.2) in the case of a regular tree, we do not repeat it here and we refer the interested reader to [3].

Proposition 4.6. *We consider a full dyadic tree $\mathcal{T}_N$ characterized by its radius* $\mathbf{r}$ *and its resistance* $\mathcal{R}$*. Supposing that the root node is at pressure* 0*, then pressures and fluxes at leaf exits are related by*

$$\mathbf{p} = B^N(\mathbf{r})\mathbf{q},\ \ B^N(\mathbf{r}) = (B^N(\mathbf{r})_{i,j})_{0\leq i,j\leq 2^N-1} \in \mathcal{M}_{2^N}(\mathbf{R}),$$

with

$$B^N(\mathbf{r})_{i,j} = \mathcal{R}_{\Pi_{0\to i+2^N}(N-\nu_{i,j})}. \tag{4.5}$$

When the pressure at the root node is $P_{root} > 0$, the relation between pressures and fluxes at leaf exits is obtained by adding P_{root} to the pressure given in Proposition 4.6.

Remark 4.7. Similarly, it is possible to express the pressure on each node according to the fluxes at the outlets using the following equalities:

$$\frac{\partial \tilde{p}_i}{\partial q_j} = \mathcal{R}_{\Pi_{0\to l+2^{[\frac{j}{2^{N-k}}]}}(k-\nu_{l,[\frac{j}{2^{N-k}}]})},$$

for $j \in \{0,...,2^N-1\}$, $i \in \{1,...,2^{N+1}-1\}$ with $i = l+2^k$.

Definition 4.8. We denote by $\mathcal{B}_N$ the set of matrices $B^N(\mathbf{r})$ which satisfy (4.5).

From the Definition 4.8, it follows that $\mathcal{B}_N$ is a subset of $S_N(\mathbf{R})$. It is also possible to give the following equivalent expression of the matrices in $\mathcal{B}_N$:

$$\begin{aligned} B^N(\mathbf{r}) \;=\; & \tilde{R}_1 I_0^N + \begin{pmatrix} \tilde{R}_2 I_1^N & 0 \\ 0 & \tilde{R}_3 I_1^N \end{pmatrix} \\ & + \begin{pmatrix} \tilde{R}_4 I_2^N & 0 & 0 & 0 \\ 0 & \tilde{R}_5 I_2^N & 0 & 0 \\ 0 & 0 & \tilde{R}_6 I_2^N & 0 \\ 0 & 0 & 0 & \tilde{R}_7 I_2^N \end{pmatrix} \\ & + ... + \begin{pmatrix} \tilde{R}_{2^N} & 0 & ... & 0 \\ 0 & \tilde{R}_{2^N+1} & 0 & 0 \\ ... & ... & ... & ... \\ 0 & 0 & 0 & \tilde{R}_{2^{N+1}-1} \end{pmatrix}, \end{aligned} \tag{4.6}$$

where 0 is used for $0I_{k(i)}^N$ with $I_{k(i)}^N \in \mathcal{M}_{2^{N-k(i)}}(\mathbf{R})$ is a matrix of ones.

Note that we also have another expression for the pressure

$$p_i = \tilde{p}_{i+2^N} = \sum_{j\in\Pi_{0\to i+2^N},} \tilde{R}_j \tilde{q}_j. \tag{4.7}$$

Remark 4.9. When the tree $\mathcal{T}_N$ is regular, the matrix $B^N(\mathbf{r})$ takes the following form, see [3]:

$$B_{i,j}^N = S_{N-\nu_{i,j}}, \tag{4.8}$$

where S_n is the cumulative resistance $R_0 + R_1 + ... + R_n$. In this case, up to a multiplicative constant, the matrix $B^N(\mathbf{r})$ is a doubly stochastic matrix which admits the Haar basis as eigenvector basis.

In the case of a non regular tree, the properties of the matrices $B^N(\mathbf{r})$ are given in Appendix A. These results will be used in the proof of Theorem 6.5.

4.3. **Tree deformation mechanism**

We are interested in the modeling of air flow in the bronchial tree and we focus on the expiration phase. In such a phase, since the pressure at the root node P_{root} is assumed to be non-negative, the pressures on the whole tree $\tilde{p}_i$ are also non-negative. More precisely, going from the root of the tree to the leaves, the pressures on a path are not decreasing. This is a consequence of the assumption that the leaf's fluxes are non-negative. Hence, the fluxes on the whole tree are also non-negative.

First, we give some technical definitions and mechanical data and then we state our main result which is Theorem 4.15.

4.3.1. *Definitions and mechanical data*

Let Φ be the total outgoing flux in the root node.

Definition 4.10. We say that a leaf flux vector $\mathbf{q} \in \mathbf{R}^{2^N}$ is ϵ-*admissible* when it satisfies ${}^tJq = \Phi$ and

$$q_i > \epsilon, \ \forall i \in \{0, ..., 2^N - 1\}. \tag{4.9}$$

We denote by Ω_ϵ the set of ϵ-admissible leaf flux vector. Moreover, we denote $\Omega = \Omega_0$ and in such a case ($\epsilon = 0$) $\mathbf{q} \in \Omega$ is simply called *admissible*.

The following lemma will be useful in order to work with strictly positive flows in every branch of the tree. This property easily comes from the Kirchhoff's law [2] applied to the fluxes at branches bifurcations.

Lemma 4.11. *Let $\Phi > 0$ be fixed and $\mathbf{q} \in \mathbf{R}^{2^N}$ be an ϵ-admissible leaf flux, then for all $i \in \{1, ..., 2^{N+1} - 1\}$, the following inequality holds*

$$2^{N-j}\epsilon < \tilde{q}_i < \Phi - (2^j - 1)\ 2^{N-j}\epsilon, \tag{4.10}$$

where $j = k(i) \in \{1, ..., N\}$ is the generation number of i.

Remark 4.12. In the sequel, we will use the following notations: $\tilde{q}_j^{min} = 2^{N-j}\epsilon$ and $\tilde{q}_j^{max} = \Phi - (2^j - 1)\ 2^{N-j}\epsilon$, with ϵ depending on Φ well-chosen, see Proposition 6.3 below.

We now study the case of an elastic dyadic tree $\mathcal{T}_N$ in which flows an incompressible, viscous and non-inertial fluid with a given total flux Φ. Similarly to Section 3, we consider three different states of the tree: *unconstrained tree*, *initial tree* and *final tree*, when every pipe of the tree has a radius which is respectively in *unconstrained*, *initial* and *final* state. We neglect the gravity and the exterior pressure is assumed to be uniform all around the tree. We denote by P_{ext}^1 and P_{ext}^2 the exterior pressures associated with the initial and final state respectively with $P_{ext}^2 \geq P_{ext}^1$.

More precisely, the *unconstrained tree*, which is denoted by $\mathcal{T}_N^0$ is such that its radius vector, denoted by $\mathbf{r}^0 \in \mathbf{R}^{2^{N+1}-1}$, satisfies:

$$t_i(\tilde{r}_i^0) = 0, \tag{4.11}$$

on every branch $\mathcal{B}_i$, $i \in \{1, ..., 2^{N+1} - 1\}$, with

$$t_i(r) = \frac{2}{5} E \tilde{r}_i^e \left(\frac{r}{\tilde{r}_i^0} - 1 \right). \tag{4.12}$$

The *initial tree*, which is denoted by $\mathcal{T}_N^e$ is such that its radius vector, denoted by $\mathbf{r}^e$ satisfies on every branch:

$$-\ t_i(\tilde{r}_i^e) + (P_0 - P_{ext}^1)\tilde{r}_i^e = 0. \tag{4.13}$$

Finally, let $\mathbf{q} \in \Omega$ be given, the *final tree*, which is denoted by $\mathcal{T}_N$ is such that its radius vector, denoted by $\mathbf{r}$, is a solution (if it exists), for all $i \geq 1$, of the following equation:

$$g_{i,\alpha_i}(\mathbf{r}, \mathbf{q}) = 0, \tag{4.14}$$

with

$$g_{i,\alpha_i}(\mathbf{r},\mathbf{q}) = \alpha_i \frac{\tilde{r}_i}{\tilde{r}_i^e} + 1 + \eta \frac{\tilde{q}_i}{\tilde{r}_i^3}, \tag{4.15}$$

and

$$\alpha_i = -1 - \frac{5\Big((P_0 - \tilde{p}_{[\frac{i}{2}]}) + (P_{ext}^2 - P_{ext}^1)\Big)}{2E} \text{ and } \eta = \frac{15C}{2E} > 0, \tag{4.16}$$

with the convention that $\tilde{p}_0 = P_{root}$.

Remark 4.13. Since α_i depends on $\mathbf{r}$ and on $\mathbf{q}$, we should denote $\alpha_i(\mathbf{r},\mathbf{q})$. Indeed in (4.16) we see that $\tilde{p}_{[i/2]}$ depends on $\tilde{r}_{[i/2]}$ and $\tilde{q}_{[i/2]}$. For simplicity we will omit this dependence.

Remark 4.14. From now on, when a tree $\mathcal{T}_N$ will be mentioned, it will be clear that it will be with an unconstrained tree $\mathcal{T}_N^0$ and with an initial tree $\mathcal{T}_N^e$.

4.3.2. *Main result*

Now, we can define the tree deformation function G by:

$$\begin{array}{rcl} G\ :]0,+\infty[^{2^{N+1}-1} \times [0,+\infty[^{2^N} & \to & \mathbf{R}^{2^{N+1}-1} \\ (\mathbf{r},\mathbf{q}) & \to & (G_i(\mathbf{r},\mathbf{q}) = g_{i,\alpha_i}(\mathbf{r},\mathbf{q}))_{1\le i\le 2^{N+1}-1}, \end{array} \tag{4.17}$$

where $g_{i,\alpha_i}(\mathbf{r},\mathbf{q})$ is given by (4.15). This is obviously a C^∞-function.

The study of the properties of G is postponed into Appendix C.1.

Theorem 4.15. *Assume that* $P_{root} < P_0 + (P_{ext}^2 - P_{ext}^1) + \frac{2E}{5}$ *and that* $\mathbf{q} \in [0,+\infty[^{2^N}$ *is such that* ${}^tJ\mathbf{q} = \Phi$. *There exists* $\mathbf{a} \in]\mathbf{0},+\infty[^{\mathbf{N}}$ *such that the following holds:*

for all tree $\mathcal{T}_N$ *satisfying* $\tilde{r}_i^e > a_{k(i)}$, *for all* $i \in \{1,...,2^{N+1}-1-2^N\}$,

there exists real numbers $\alpha_1^{min} < \alpha_1^{max} < 0$ *such that*

for all $\alpha_1 \in]\alpha_1^{min};\alpha_1^{max}[$, *there exists a unique solution of* $G(\mathbf{r},\mathbf{q}) = 0$,

with G *given by* (4.17). *This solution is denoted by* $\mathbf{r}^\alpha(\mathbf{q}) = (\tilde{r}_i^{\alpha_i}(\tilde{q}_i))_{i\in\{1,...,2^{N+1}-1\}}$.

Furthermore, there exists strictly positive real numbers $(\tilde{r}_j^{min},\tilde{r}_j^{max})_{1\le j\le N}$ *such that for all* i *in* $\{1,...,2^{N+1}-1\}$*:*

$$\tilde{r}_j^{min} \le \tilde{r}_i^{\alpha_i}(\tilde{q}_i) \le \tilde{r}_j^{max}, \tag{4.18}$$

with $j = k(i)$.

Moreover the function $\mathbf{q} \to \mathbf{r}^\alpha(\mathbf{q})$ *is* C^∞ *for* $\mathbf{q} \in [0,\Phi]^{2^N}$.

Proof. We will proceed recursively on the generations. Let $\mathcal{T}_N$ be a tree of height N. Recalling Proposition 3.5, condition (3.14) with $P_a = P_{root}$ is exactly the hypothesis $P_{root} < P_0 + (P_{ext}^2 - P_{ext}^1) + \frac{2E}{5}$, hence we know that there exists real numbers $\alpha_1^{min} < \alpha_1^{max} < 0$ such that for all $\alpha_1 \in]\alpha_1^{min};\alpha_1^{max}[$, there exists a unique solution, denoted by $r_1^{\alpha_1}(\mathbf{q})$, of $g_{1,\alpha_1}(\mathbf{r},\mathbf{q}) = 0$. Moreover, recalling Remark 3.7, we deduce that

$$\tilde{p}_1^{min} \le \tilde{p}_1 \le \tilde{p}_1^{max} \tag{4.19}$$

where

$$\tilde{p}_1^{min} = P_{root} + 6C\frac{\tilde{r}_1^e}{\left(\tilde{r}_1^{max}\right)^4}\tilde{q}_1^{min} \text{ and } \tilde{p}_1^{max} = P_{root} + 6C\frac{\tilde{r}_1^e}{\left(\tilde{r}_1^{min}\right)^4}\tilde{q}_1^{max}, \tag{4.20}$$

with

$$\tilde{r}_1^{min} = \tilde{r}_1^{\alpha_1,min}(\mathbf{q}) = \tilde{r}_1^{\alpha_1^{min}}(\Phi) \text{ and } \tilde{r}_1^{max} = \tilde{r}_1^{\alpha_1,max}(\mathbf{q}) = \tilde{r}_1^{\alpha_1^{max}}(\Phi). \tag{4.21}$$

Next, we want to obtain α_2^{min} and α_2^{max} such that $\alpha_2^{max} < 0$ and

$$\alpha_2^{min} \leq \alpha_2 \leq \alpha_2^{max} \text{ along with } \alpha_2^{min} \leq \alpha_3 \leq \alpha_2^{max} \tag{4.22}$$

where

$$\begin{aligned} \alpha_2^{min} &= -1 - \frac{5\Big((P_0 - \tilde{p}_1^{min}) + (P_{ext}^2 - P_{ext}^1)\Big)}{2E}, \\ \alpha_2^{max} &= -1 - \frac{5\Big((P_0 - \tilde{p}_1^{max}) + (P_{ext}^2 - P_{ext}^1)\Big)}{2E}. \end{aligned}$$

Inequality $\alpha_2^{max} < 0$ is equivalent to

$$\tilde{p}_1^{max} < P_0 + (P_{ext}^2 - P_{ext}^1) + \frac{2E}{5}. \tag{4.23}$$

There are two alternative situations:

- The inequality (4.23) is verified, we choose $a_1 = r_1^e$ and we can go on to the next step.
- The inequality (4.23) is false. According to Proposition 3.6, $\tilde{r}_1^{min} \overset{\tilde{r}_1^e \to +\infty}{\sim} -\tilde{r}_1^e/\alpha_1^{min}$. This implies that $\tilde{r}_1^e/(\tilde{r}_1^{min})^4$ goes to zero when $\tilde{r}_1^e$ goes to infinity. Thus, $\tilde{p}_1^{max}$ goes to P_{root} when $\tilde{r}_1^e$ goes to infinity, hence there exists $a_1 > 0$ such that if $\tilde{r}_1^e > a_1$ then $\tilde{p}_1^{max} < P_0 + (P_{ext}^2 - P_{ext}^1) + \frac{2E}{5}$.

Note that the second situation can be reproduced in the downward parts of the tree because the pressure in one node only depends on what happens between this branch and the root of the tree. Hence, the next steps, modifying only downward branches in the tree, will not modify the properties (pressure, flow or radius) of the current branch. Therefore, reproducing this scheme in the next generations of the tree leads to the existence of a real vector $\mathbf{a} = (\mathbf{a_i})_{\mathbf{i=0},\ldots,\mathbf{N-1}}$ such that if, for all i verifying $k(i) = j$, $\tilde{r}_i^e > a_j$, then $\tilde{p}_j^{max} < P_0 + (P_{ext}^2 - P_{ext}^1) + \frac{2E}{5}$ and $\alpha_j^{max} < 0$. Finally, note that no similar condition need to be imposed to the last 2^N generation branches.

Hence, following this approach recursively, we obtain the result. □

Remark 4.16. In Theorem 4.15, the real numbers $(\alpha_k^{min}, \alpha_k^{max})_{1 \leq k \leq N}$ are constructed in such a way that for all i in $\{1, \ldots, 2^{N+1} - 1\}$:

$$\alpha_j^{min} \leq \alpha_i \leq \alpha_j^{max} \leq 0, \tag{4.24}$$

with $j = k(i)$.

In this study, the geometry of the tree is defined through its initial state and more precisely through P_0, P_{ext}^1, E and its initial radii $\mathbf{r}^e$, thus $\mathbf{r}^e$ is a data as much as E is. Moreover, the unconstrained radius $\mathbf{r}^0$ is a consequence of those data, and in particular of $\mathbf{r}^e$. This choice of data has been driven by the method used in [12,13] in order to measure sizes in lungs, actually measurements have been made in a state close to end inspiration at rest regime. Indeed, it is the reason why we choose to impose hypothesis on $\mathbf{r}^e$ in Theorem 4.15.

The previous theorem leads to the definition of the function $\mathbf{q} \to \mathbf{r}^\alpha(\mathbf{q})$.

Definition 4.17. Under the same assumptions as Theorem 4.15, we define the C^∞ mapping $\mathbf{r}^\alpha$ as follows:

$$\begin{aligned} \mathbf{r}^\alpha \ : \ [0;\Phi]^{2^N} &\to \prod_{j=1}^{2^{N+1}-1}]\tilde{r}_j^{min}; \tilde{r}_j^{max}[^{2^j} \\ \mathbf{q} &\to \mathbf{r}^\alpha(\mathbf{q}) \end{aligned}$$

such that $G(\mathbf{r}^\alpha(\mathbf{q}), \mathbf{q}) = 0$.

From now on, we will assume that the real numbers $\alpha_1^{min} < \alpha_1^{max} < 0$ are fixed and we will simply note $\mathbf{r} = \mathbf{r}^\alpha$.

5. Viscous energy minimization

Let $\mathcal{T}_N$ be given and $B^N(\mathbf{r})$ be the resistance matrix associated to it by Proposition 4.6 and Definition 4.8. We recall that $B^N(\mathbf{r})$ is a real symmetric matrix of size $2^N \times 2^N$.

Let us denote by E_D the viscous dissipated energy of the tree. It is a function of the flux vector $\mathbf{q}$ at leaves, and it is the sum of the viscous dissipated energy in each branch of the tree (for the branch i, this loss of energy is $\tilde{R}_i \tilde{q}_i^2$). It is easy to prove that the total viscous dissipated energy in the tree is given by

$$E_D(\mathbf{q}) = {}^t\mathbf{q} B^N(\mathbf{r}) \mathbf{q}.$$

Assuming that the flow Φ going through the first generation branch (the root node or the "trachea" depending on which part of the human lung we consider) is given, we want to minimize E_D over all fluxes $\mathbf{q} \in [0;\Phi]^{2^N}$ such that

$$F(\mathbf{q}) = {}^tJ\mathbf{q} = \Phi,$$

where we recall that $J = {}^t(1,1,...,1)$.

Using Lagrange multipliers, at an extremum $\mathbf{q}^0$, we have

$$\nabla E_D(\mathbf{q}^0) = \lambda \nabla F(\mathbf{q}^0),$$

hence, for all h in $\mathbf{R}^{2^N}$, $2{}^t\mathbf{q}^0 B^N(\mathbf{r}) h = \lambda {}^t J h$.

Therefore, we have:

$$\begin{aligned} 2B^N(\mathbf{r})\mathbf{q}^0 &= \lambda J, \\ {}^tJ\mathbf{q}^0 &= \Phi, \end{aligned}$$

whence $\mathbf{q}^0 = \frac{\lambda}{2}(B^N(\mathbf{r}))^{-1}J$ and $\Phi = \frac{\lambda}{2}\,{}^tJ(B^N(\mathbf{r}))^{-1}J$, this gives $\lambda = 2\Phi/{}^tJ(B^N(\mathbf{r}))^{-1}J$ and

$$\mathbf{q}^0 = \frac{(B^N(\mathbf{r}))^{-1}J}{{}^tJ(B^N(\mathbf{r}))^{-1}J} \times \Phi.$$

Remark 5.1. In particular, the optimal flow $\mathbf{q}_0$ is the image of an homogeneous distribution of pressures at exits equal to $\Phi/({}^tJB^N(\mathbf{r})^{-1}J)$ (note that the term $({}^tJB^N(\mathbf{r})^{-1}J)^{-1}$ represents the equivalent hydrodynamic resistance of the whole tree).

Remark 5.2. Note that if $\mathcal{T}_N$ is homogeneous, see Remark 4.9, J is an eigenvector of A and $\mathbf{q}^0 = \Phi/2^N\ J$.

Let us now define a flux optimization mapping as follows:

Definition 5.3. Let $\mathcal{T}_N$ be given and $B^N(\mathbf{r})$ be its resistance matrix (see Prop. 4.6), the mapping f is defined as follows:

$$\begin{aligned} f\ :]0,+\infty[^{2^{N+1}-1} &\to \mathbf{R}^{2^N} \\ \mathbf{r} &\to f(\mathbf{r}) = \mathbf{q}^0 = Q\ o\ \left(B^N(\mathbf{r})\right) = \frac{(B^N(\mathbf{r}))^{-1}J}{{}^tJ(B^N(\mathbf{r}))^{-1}J}\Phi, \end{aligned} \tag{5.1}$$

with Q defined by:

$$\begin{aligned} Q\ :\ S_{2^N}^{+*}(\mathbf{R}) &\to \mathbf{R}^{2^N} \\ A &\to Q(A) = \frac{A^{-1}J}{{}^tJA^{-1}J}\Phi. \end{aligned}$$

We recall that $\Omega = \{\mathbf{q} \in]0;\Phi[^{2^N} \text{ such that } {}^tJ\mathbf{q} = \Phi\}$. Moreover, the proof of the fact that $B^N(\mathbf{r})$ belongs to the set $S_{2^N}^{+*}(\mathbf{R})$ is given in Appendix C.1.

Proposition 5.4. *The mapping f satisfies $Im(f) \subset \Omega$.*

Proof. Since ${}^tJf(\mathbf{r}) = \Phi$, it is enough to prove that $f(\mathbf{q})_i > 0$, for all $i \in \{0, ..., 2^N - 1\}$. This easily follows from Lemma A.2. □

6. Optimization flux for a deformable tree

In this section, we state our main result in Theorem 6.5. Since the proof is technical, we postpone it until Appendix C.

We consider an elastic dyadic tree $\mathcal{T}_N$ with given radii $\mathbf{r}^0$ and $\mathbf{r}^e$, we prove that under some assumptions on $\alpha_1(\mathbf{r}, \mathbf{q})$, there exists an optimal flux $\mathbf{q} \in \Omega$ for the deformed tree of radius $\mathbf{r}(\mathbf{q})$ given by Definition 4.17.

Proposition 6.1. *Under the same assumptions as Theorem 4.15, there exists $\mathbf{q}_F$ in Ω such that*

$$F(\mathbf{q}_F) = \mathbf{q}_F,$$

where F is defined by

$$\begin{array}{rccl} F & : & \overline{\Omega} & \to & \Omega \\ & & \mathbf{q} & \to & F(\mathbf{q}) = \dfrac{\left(B^N(\mathbf{r}(\mathbf{q}))\right)^{-1} J}{{}^tJ\left(B^N(\mathbf{r}(\mathbf{q}))\right)^{-1} J}\Phi = f \circ \mathbf{r}(\mathbf{q}). \end{array}$$

Proof. Since $Im(F) \subset \Omega \subset \overline{\Omega}$ and $\overline{\Omega}$ is a compact and convex set and because F is continuous, from the Brouwer fixed point theorem, we deduce the existence of $\mathbf{q}_F \in \overline{\Omega}$ such that $F(\mathbf{q}_F) = \mathbf{q}_F$. Because $Im(F) \subset \Omega$, it follows that $\mathbf{q}_F \in \Omega$. □

Remark 6.2. Recalling Remark 5.1, we know that optimal flow corresponds to identical pressures at each exit. Hence, it is also possible to search optimal pressure $p \in \mathbf{R}$ of deformed tree exits through a fixed point of the application

$$H(p) = \left({}^tJ\left(B^N\left(\mathbf{r}(B^N(\mathbf{r}_0)^{-1}pJ)\right)\right)^{-1}J\right)^{-1}\Phi.$$

However, to obtain branch deformation it is necessary to compute the flow vector $\mathbf{q} = B^N(\mathbf{r}_0)^{-1}pJ$ and complexity of both approaches are the same.

It is possible to obtain a better localization of the fixed point $\mathbf{q}_F$ using the fact that for each tree $\mathcal{T}_N$ there exists $\epsilon_{\mathcal{T}_N} > 0$ such that $Im(F) \subset \Omega_{\epsilon_{\mathcal{T}_N}}$. This property is a consequence of the limitation of deformation range of radii. Actually, and because the fluxes are bounded by Φ and positive, the tree branches cannot collapse (zero radius) or infinitely dilate.

Proposition 6.3. *Under the same assumptions as Theorem 4.15, there exists $\epsilon_{\mathcal{T}_N} > 0$ such that $Im(F) \subset \Omega_{\epsilon_{\mathcal{T}_N}}$.*

Proof. Let us define the application $m : \Omega \to]0;\Phi[$ such that $m(\mathbf{q}) = \min_i \mathbf{q}_i$. The application m is continuous on Ω along with F on $\overline{\Omega}$. Hence the applications $m \circ F$ is continuous on the compact $\overline{\Omega}$. Then $m \circ F$ reaches its minimum η in $\overline{\Omega}$ and because $F(\mathbf{q})_i > 0$ for each $\mathbf{q} \in \overline{\Omega}$, $\eta > 0$. Taking $\epsilon_{\mathcal{T}_N} = \eta/2$ leads to the result by definition, because $F(\mathbf{q})_i > \epsilon_{\mathcal{T}_N}$ for each $\mathbf{q} \in \overline{\Omega}$. □

Finally, the following result holds:

Proposition 6.4. *Under the same assumptions as Theorem 4.15, the restriction $F_{|\Omega_{\epsilon_{\mathcal{T}_N}}}$ of F on $\Omega_{\epsilon_{\mathcal{T}_N}}$ admits a flow $\mathbf{q}_F \in \Omega_{\epsilon_{\mathcal{T}_N}}$ such that $F_{|\Omega_{\epsilon_{\mathcal{T}_N}}}(\mathbf{q}_F) = \mathbf{q}_F$.*

Proof. Using $\overline{\Omega_{\epsilon_{\mathcal{T}_N}}}$ in the same way than Proposition 6.1 leads to the result. □

According to Remark 4.12, we will use $\epsilon_{\mathcal{T}_N}$ as ϵ to define the different values of q_j^{min} and q_j^{max}.

The preceding result does not give uniqueness and can not be easily used to build a fixed point. However with stronger hypothesis, Picard's theorem applies and can be used to numerically estimate the fixed point. This leads to the following theorem. Note that its proof is quite technical and can be found in the Appendix C.

Theorem 6.5. *Assuming Theorem 4.15 hypothesis, there exists $\eta > 0$ such that if Φ belongs to $[0, \eta[$ then the Picard fixed-point theorem applies for F on $\Omega_{\epsilon_{\mathcal{T}_N}}$. This leads to uniqueness of the fixed point $\mathbf{q}_F$ of F in $\Omega_{\epsilon_{\mathcal{T}_N}}$ and to convergence toward $\mathbf{q}_F$ of the scheme:*

$$\mathbf{q}_0 = \mathbf{q} \in \Omega_{\epsilon_{\mathcal{T}_N}}, \ \mathbf{q}_{n+1} = F(\mathbf{q}_n). \tag{6.1}$$

7. Numerical simulations

7.1. Methodology

The simulations are applications of Theorem 6.5. They were performed with Matlab 7. The evaluations of the function $\mathbf{q} \to \mathbf{r}(\mathbf{q})$, defined by $G(\mathbf{r}(\mathbf{q}), \mathbf{q}) = 0$ (Thm. 4.15), were obtained through a Newton method. The numerical process uses the characteristic geometrical structure of this problem and calculates most of the different variables (pressures, radii) from the top of the tree down to the lower part. Numerical values for the different parameters were obtained from lung physiology literature [1,4,9,11–13,15] and will not be discussed here. Young's modulus is assumed to be constant along the generations. Although this last hypothesis is not quite realistic, applying a mean value to the whole tree seems a good compromise knowing that mechanical properties of small bronchi are not well known. Thus, we use $E = 6250$ Pa for Young's modulus [9,11] of each bronchi walls. The tree is assumed to have eleven generations and to be of fractal structure: bronchi of one generation are homothetic to bronchi of the previous generation with a factor $h = 0.82$ [7,12,14]. Parenchyma pressures have been fitted relatively to trachea velocities from measures obtained in [4].

To measure the global deformation of the structure, the mean l^2-deformation of the branches or tree deformation (%) will be used. It is given by:

$$d = \frac{100}{2^{N+1}-1}\sqrt{\sum_{i=1}^{2^{N+1}-1}\left(\frac{r_i - r_i^e}{r_i^e}\right)^2}.$$

7.2. Convergence

To study the convergence speed of Proposition 6.1, a local estimate of the Lipschitz constant k of the application F has been calculated. Convergence velocity is given by the following inequality, which holds true for all $n \in \mathbb{N}^*$:

$$||\mathbf{q}_n - \mathbf{q}||_2 \leq \frac{k^n}{1-k}||\mathbf{q}_1 - \mathbf{q}_0||_2.$$

To locally estimate k, the value $Err = \ln\left((\mathbf{q}_{n+1} - \mathbf{q}_n)/(\mathbf{q}_1 - \mathbf{q}_0)\right)$ has been stored for each sequence index n. According to the inequality $||\mathbf{q}_{n+1} - \mathbf{q}_n||_2 \leq k^n||\mathbf{q}_1 - \mathbf{q}_0||_2$ going along with Picard theorem, if convergence occurs, Err should be smaller than a line with negative slope $ln(k)$ ($k \in]0, 1[$) and hence should be decreasing to $-\infty$ with n.

To illustrate the scheme convergence, we exhibit an example corresponding to the tree described previously (Sect. 7.1), but one of its third generation branches is assumed to be partly collapsed (the radius has been reduced to one third of its original value). The flow and root pressure have been adjusted such that the velocity in trachea corresponds to forced expiration and reaches 15 $\mathrm{m \cdot s^{-1}}$ (remember that the first generation of our tree corresponds to the sixth generation of the lung). The Young modulus has been chosen to be $E = 1250$ Pa (five times smaller than in the previous section). The results are presented on Figure 4. On the left part Err

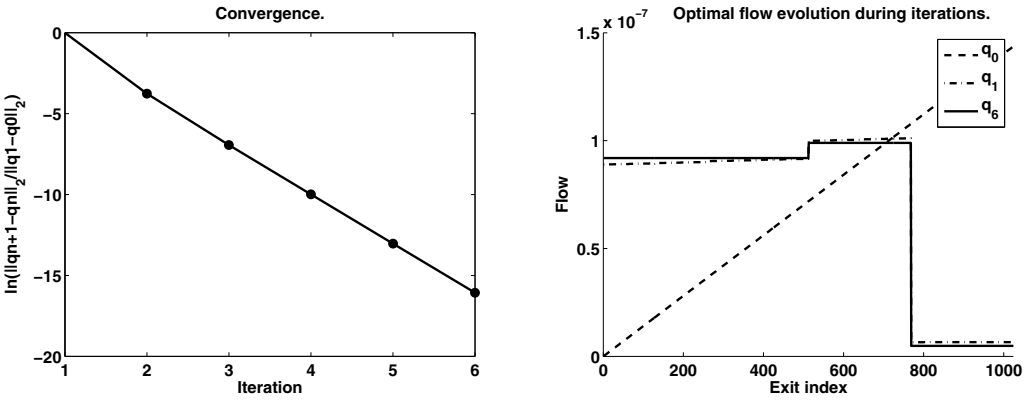

FIGURE 4. Convergence of iterative scheme $q_{n+1} = F(q_n)$. Left: "convergence curve" (ln of relative error from one step to the next), this curve helps us to bound the Lipschitz constant of F, which is smaller than 0.042 here, hence the convergence is fast. Right: flow during iterative scheme, initial flow $\mathbf{q}_0$ is represented by the dashed line.

has been represented and is decreasing very fast. From the numerical results, the local Lipschitz constant is smaller than 0.042. Hence for the sixth iteration, the inequality $||\mathbf{q}_6 - \mathbf{q}||_2 \leq 1.3 \times 10^{-7}||\mathbf{q}_1 - \mathbf{q}_0||_2$ holds. The right part of Figure 4 shows the leaf flow profile in the tree along the iterative process. Since the convergence is fast, the difference between the initial profile (dashed line) and the first iteration profile (dashed dotted line) is large. The sixth iteration (continuous line) is very close to optimal flow.

The mean l^2 deformation of the branches in this example is of 17.6%, with a larger value reached on a leaf branch (17.9%) and smaller value on root branch (14.8%). The dissipated viscous energy in the tree with flow $\mathbf{q}_6$ represents only 13.6% of the dissipated energy with flow $\mathbf{q}_0$.

Note that as stated in Proposition C.3, reducing too much the parameter E (lower than 223 Pa in this particular case, to compare to the 6250 Pa for the lung) or increasing too much the parameter Φ (trachea velocity larger than 77 $\mathrm{m} \cdot \mathrm{s}^{-1}$) leads to non convergent schemes. Moreover, these two thresholds depend on each other, for instance a 70 $\mathrm{m} \cdot \mathrm{s}^{-1}$ velocity in the trachea leads to a threshold on E of 1087 Pa, while $E = 6250$ Pa leads to a threshold on trachea velocity of 234 $\mathrm{m} \cdot \mathrm{s}^{-1}$).

7.3. **Study of equal pressure point (EPP)**

The behavior of bronchial wall (constricted or dilated) is defined by the difference between pressure increases in the bronchia and in the parenchyma (pleural pressure). There are two scenarii:

- This difference is negative, this leads to bronchial dilatation.
- This difference is positive, this leads to bronchial constriction.

From the leaves of the tree to its root, the bronchial pressure $\mathbf{p}_i$ decreases with generations up to the trachea, where it reaches atmospheric pressure (chosen to be 0 in our model). In the case when pleural pressure increase during expiration is lower than alveolar pressure increase, then both scenarii can happen in different bronchi of the tree. This creates a dilated region in the lower part of the tree and a constricted region in the higher part, as shown on Figure 5. The transition region (which is more precisely a set of generations in our model) is called the *equal pressure point*, shortly named EPP.

To track EPP, we have simulated a range of velocities in trachea and checked when both scenarii are present, using the following property. The tree deformation is directly linked to the presence of EPP: deformation reaches its minima when EPP reaches in the tree. This is a natural consequence of its definition. Actually, pressure in the branches where EPP occurs is at equilibrium with parenchyma pressure and these branches are

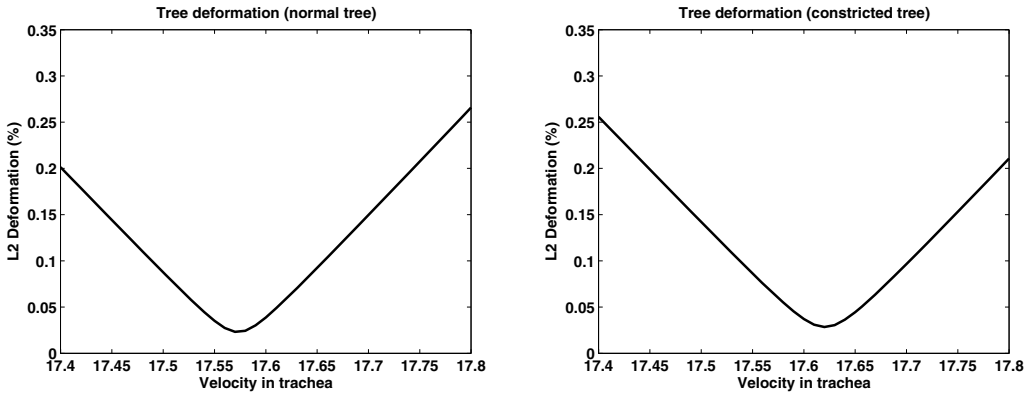

FIGURE 5. Plots of tree deformations. The minimum point is used to localize the range of velocities where EPP occurs. On the left: a fractal tree of eleven generations ($h = 0.82$), on the right: the same fractal tree with a branch from the third generation being partly collapsed (radius divided by three). Note the effect of this collapse on EPP localization.

not deformed. Thus, pressure in the other branches are the closest to equilibrium with parenchyma than in any other configuration and the whole tree suffers the smallest deformations. Hence we have used this criterion to detect EPP.

Two tree deformations plots for a range of trachea velocity have been drawn on Figure 5. The left plot corresponds to a fractal tree of eleven generation ($h = 0.82$) and shows a minima around 17.57 $\mathrm{m} \cdot \mathrm{s}^{-1}$. The right plot shows the consequence on the minima on a tree with a third generation branch partly collapsed (radius divided by three). The minima is then shifted to the higher velocity 17.62 $\mathrm{m} \cdot \mathrm{s}^{-1}$. Hence the global deformation can be linked to tree structure or defects, this criterion could be used to check tree pathologies due to geometrical changes.

A. Appendix: Properties of matrices $B^N(\mathbf{r}) \in \mathcal{B}_N$

In this appendix, we give some properties of the set $\mathcal{B}_N$ of matrices $B^N(\mathbf{r})$ given by (4.5) which will be useful in the calculation of estimates on the eigenvalues and on the inverse of matrices B^N.

The first result is a direct consequence of the formulation (4.6) of the matrices B^N together with the semi-definite positive character of I_k^N, $0 \leq k \leq N-1$, and of the diagonal matrix

$$\begin{pmatrix} \tilde{R}_{2^N} & 0 & ... & 0 \\ 0 & \tilde{R}_{2^N+1} & 0 & 0 \\ ... & ... & ... & ... \\ 0 & 0 & 0 & \tilde{R}_{2^{N+1}-1} \end{pmatrix}.$$

Proposition A.1. *Let $B^N(\mathbf{r}) \in \mathcal{B}_N$, then it is positive definite and its eigenvalues $\lambda_0, ..., \lambda_{2^N-1}$ satisfy:*

$$\begin{aligned} \min_{i\in\{0,...,2^N-1\}} \lambda_i &\geq \min(\tilde{R}_{2^N}, \tilde{R}_{2^N+1}, ..., \tilde{R}_{2^{N+1}-1}), \\ \max_{i\in\{0,...,2^N-1\}} \lambda_i &\leq 2^N \tilde{R}_1 + 2^{N-1} \max(\tilde{R}_2, \tilde{R}_3) + ... + \max(\tilde{R}_{2^N}, \tilde{R}_{2^N+1}, ..., \tilde{R}_{2^{N+1}-1}). \end{aligned}$$

The following result shows that the relation $\mathbf{p} = B^N(\mathbf{r})\mathbf{q}$ is invertible. Therefore, one can choose indifferently pressures or fluxes at leaves to study the structure of the flow in the tree. The inequality given in the following lemma is needed in order to prove Proposition 5.4.

Lemma A.2. *The set $\mathcal{B}_N$ is a subset of $GL_{2^N}(\mathbf{R})$. Moreover, let $B^N(\mathbf{r})$ belongs to $\mathcal{B}_N$, then*

$$\Big(B^N(\mathbf{r})^{-1}J\Big)_i > 0,\ \forall i \in \{0,...,2^N-1\}.$$

Proof. Since $B^N(\mathbf{r})$ is a positive definite matrix, it belongs to $GL_{2^N}(\mathbf{R})$.

Let $(B^N(\mathbf{r}))^{-1}J = {}^t(\beta_0,...,\beta_{2^N-1})$. From $B^N(\mathbf{r})(B^N(\mathbf{r}))^{-1}J = J$ together with the Definition 4.6 of $B^N(\mathbf{r})$, we easily deduce that

$$\Big(B^N(\mathbf{r})(B^N(\mathbf{r}))^{-1}J\Big)_0 - \Big(B^N(\mathbf{r})(B^N(\mathbf{r}))^{-1}J\Big)_1 = \tilde{R}_4\beta_0 - \tilde{R}_5\beta_1 = 0,$$

hence $\beta_0\beta_1 \geq 0$ and $\beta_0\beta_1 = 0$ if and only if $\beta_0 = \beta_1 = 0$. Similarly, we obtain that $\beta_{2i}\beta_{2i+1} \geq 0$ and $\beta_{2i}\beta_{2i+1} = 0$ if and only if $\beta_{2i} = \beta_{2i+1} = 0$ for all $i \in \{0,...,2^{N-1}-1\}$.

Moreover, we also have

$$\Big(B^N(\mathbf{r})(B^N(\mathbf{r}))^{-1}J\Big)_0 - \Big(B^N(\mathbf{r})(B^N(\mathbf{r}))^{-1}J\Big)_2 = \tilde{R}_4\beta_0 - \tilde{R}_9\beta_2 + \tilde{R}_2(\beta_0+\beta_1) - \tilde{R}_3(\beta_2+\beta_3) = 0.$$

Using next that $\beta_1 = \frac{\tilde{R}_4}{\tilde{R}_5}\beta_0$ and $\beta_3 = \frac{\tilde{R}_6}{\tilde{R}_7}\beta_2$, we obtain

$$\Big(\tilde{R}_2 + \tilde{R}_4 + \frac{\tilde{R}_2}{\tilde{R}_5}\tilde{R}_4\Big)\beta_0 = \Big(\tilde{R}_3 + \tilde{R}_6 + \frac{\tilde{R}_6}{\tilde{R}_{11}}\tilde{R}_3\Big)\beta_2,$$

hence $\beta_0\beta_2 \geq 0$ and $\beta_0\beta_2 = 0$ if and only if $\beta_0 = \beta_2 = 0$. Similarly, we obtain that $\beta_{2i}\beta_{2i+2} \geq 0$ and $\beta_{2i}\beta_{2i+2} = 0$ if and only if $\beta_{2i} = \beta_{2i+2} = 0$ for all $i \in \{0,...,2^{N-1}-2\}$.

Hence, following this approach recursively, from

$$\Big(B^N(\mathbf{r})(B^N(\mathbf{r}))^{-1}J\Big)_i - \Big(B^N(\mathbf{r})(B^N(\mathbf{r}))^{-1}J\Big)_j = 0,$$

we deduce that all the β have the same sign and if one of them vanishes, so do all of the others. The latter case is not possible since $B^N(\mathbf{r})^t(\beta_0,...,\beta_{2^N-1}) = J$. Moreover from $B^N(\mathbf{r})^t(\beta_0,...,\beta_{2^N-1}) = J$ again, we deduce that $\beta_i > 0$. □

B. Appendix: Properties of path matrices

In this appendix, we give the definition and properties of a particular set of matrix denoted by $\mathcal{P}_{2^{N+1}-1}$. The results describe here will be used for the estimates of Appendix C which are necessary in order to prove Theorem 6.5.

Definition B.1. Let $\mathcal{P}_{2^{N+1}-1}$ be the set of square matrices defined by:

$$\begin{aligned}\mathcal{P}_{2^{N+1}-1} \quad = \quad & \Big\{P \in GL_{2^{N+1}-1}(\mathbf{R}) \text{ such that } P \text{ is lower triangular and} \\ & P_{ij} = 0 \text{ if } j \notin \Pi_{0\to i},\ i,j \in \{1,...,2^{N+1}-1\}\Big\}.\end{aligned}$$

Example 1. The gradient matrix $\nabla_{\mathbf{q}_{\mathcal{T}_N}}\mathbf{p}_{\mathcal{T}_N}(\mathbf{q}_{\mathcal{T}_N})$ of the application $\mathbf{q}_{\mathcal{T}_N} \to \mathbf{p}_{\mathcal{T}_N}(\mathbf{q}_{\mathcal{T}_N})$ belongs to $\mathcal{P}_{2^N}$.

Let us now establish some properties of matrices belonging to the set $\mathcal{P}_{2^{N+1}-1}$. This set and its property will be useful in the sequel to study the convergence speed of an iterative process, see Appendix C.

Proposition B.2. *Let A belongs to $\mathcal{P}_{2^{N+1}-1}$, then A^{-1} belongs to $\mathcal{P}_{2^{N+1}-1}$.*

Actually, $(\mathcal{P}_{2^{N+1}-1}, \times)$ is a subgroup of $GL_{2^{N+1}-1}(\mathbf{R})$. Moreover the inverse of an element of $\mathcal{P}_{2^{N+1}-1}$ can be obtained through an iterative process (it can be built column-wise, from the beginning of the column to the end):

Proposition B.3. *Let $A = (a_{ij}) \in \mathcal{P}_{2^{N+1}-1}$ then its inverse $B = (b_{ij}) \in \mathcal{P}_{2^{N+1}-1}$ is such that:*

$$b_{ij} = \left(\frac{-1}{a_{ii}}\right) \left(\sum_{k \in \Pi_{0\to i} \setminus \Pi_{0\to j}, k \neq i} a_{ik} b_{kj} \right) \text{ for } j \in \Pi_{0\to i},\ j \neq i$$

and

$$b_{ii} = \frac{1}{a_{ii}} \text{ for } i \in \{1, ..., 2^{N+1} - 1\}.$$

Proof. We easily see that B belongs to $\mathcal{P}_{2^{N+1}-1}$ and that $AB = I_{2^{N+1}-1}$. □

Now we obtain an upper bound for the coefficients of $A^{-1} = (b_{ij})$ depending on boundary properties on the coefficients of the matrix A in $\mathcal{P}_{2^{N+1}-1}$. Let $A = (a_{ij})$ be given in $\mathcal{P}_{2^{N+1}-1}$. We assume uniform boundedness conditions:

$$\forall i \neq j,\ |a_{ij}| \leq \alpha \text{ and } -a_{ii} \geq \beta > 0. \tag{B.1}$$

First let us introduce the following real sequence:

$$\begin{cases} u_1 = 1/\beta \\ u_{n+1} = \frac{\alpha}{\beta} \sum_{p=1}^{n} u_p. \end{cases}$$

Lemma B.4. *This sequence can be rewritten for $n \geq 2$:*

$$u_n = \left(1 + \frac{\alpha}{\beta}\right)^{n-2} \frac{\alpha}{\beta^2}.$$

Proof. We have $u_{n+1} - u_n = (\alpha/\beta)u_n$ for $n \geq 2$, hence using $u_2 = \alpha/\beta^2$ gives the result. □

Proposition B.5. *Let i, j in $\{1, ..., 2^{N+1} - 1\}$ be such that $i \geq j$.*

According to the branch numbering, this implies that the corresponding generations of the branch i and j verify $k(i) \geq k(j)$. With this hypothesis, we have:

$$|b_{ij}| \leq u_{(k(i)-k(j)+1)}.$$

Proof. Let i, j be in $\{1, ..., 2^{N+1} - 1\}$ such that $i \geq j$.

Let $\Pi_{j\to i}$, for $i \geq j$, be defined as follows:

$$\begin{aligned} \Pi_{j\to i} &= \emptyset && \text{if } j \notin \Pi_{0\to i}, \\ &= \Pi_{0\to i} \setminus \Pi_{0\to j} && \text{if } j \in \Pi_{0\to i}. \end{aligned}$$

If $\Pi_{j\to i} = \emptyset$ then $b_{ij} = 0$ and the inequality is true.

Now assume $\Pi_{j\to i} \neq \emptyset$.

According to the definition of b_{ij} and the boundedness hypothesis on α_{ij}, we can write if $i \neq j$:

$$|b_{ij}| \leq \frac{\alpha}{\beta} \sum_{p \in \Pi_{j\to i}, p \neq i} |b_{pj}|$$

and of course $b_{ii} \leq 1/\beta$.

The important point is that the set of b_{pj} corresponds to the branches linking branch j of generation $k(j)$ branch i of generation $k(i)$. Hence there is exactly one p in the sum for each generation in $\{k(j), k(j)+1, ..., k(i)-1\}$ (recall that we suppose $p \neq i$). Therefore, there are exactly $k(i)-k(j)$ terms in the sum. This also shows that the upper bound of b_{ij} only depends of b_{pj} which have smaller generations and consequently such that their indexes p verify $p < i$.

Hence, we will use a recursive proof indexed by the difference between generations $k(i)-k(j)$. Recall that we assume $\Pi_{j\to i} \neq \emptyset$.

The n ranked induction hypothesis is: "if $k(i)-k(j) \leq n$ then $b_{ij} \leq u_{k(i)-k(j)+1}$".

Assume first $k(i)-k(j)=0$, this means $i=j$ and

$$|b_{ii}| = \frac{1}{|a_{ii}|} \leq \frac{1}{\beta} = u_1.$$

This is true at rank 0.

Now assume $k(i)-k(j)=n+1$ and assume true the n ranked induction hypothesis, then:

$$|b_{ij}| \leq \frac{\alpha}{\beta} \sum_{m\in\Pi(j\to i), m\neq i} |b_{mj}|.$$

But we recall that if m is different from i and belongs to the set $\Pi_{j\to i}$, its associated generation is smaller than i, hence $k(m)-k(j) < k(i)-k(j)$ and $k(m)-k(j) \leq n$. Moreover such m, (*i.e.* different from i and belonging to the set $\Pi_{j\to i}$), cover each generations between $k(j)$ and $k(i)-1$. Consequently for each p in $\{k(j), ..., k(i)-1\}$ there exists a unique m_p in the sum such that $k(m_p)=p$. According to the n ranked induction hypothesis we have:

$$|b_{m_p j}| \leq u_{k(m_p)-k(j)+1}.$$

Now putting this in b_{ij}:

$$|b_{ij}| \leq \frac{\alpha}{\beta} \sum_{p=k(j)}^{k(i)-1} |b_{m_p j}| \leq \frac{\alpha}{\beta} \sum_{p=k(j)}^{k(i)-1} u_{k(m_p)-k(j)+1}$$

which leads to:

$$|b_{ij}| \leq \frac{\alpha}{\beta} \sum_{p=1}^{k(i)-k(j)} u_p = \frac{\alpha}{\beta} \sum_{p=1}^{n+1} u_p = u_{n+2}.$$

This shows the $n+1$ ranked induction hypothesis and the result is true for every $n \in \mathbb{N}^*$. □

Now if the tree has N generations and because $n \to u_n$ is increasing, we have:

$$|b_{ij}| \leq \left(1+\tfrac{\alpha}{\beta}\right)^{N-2} \tfrac{\alpha}{\beta^2} \quad \text{for } i \neq j,$$

$$|b_{ii}| \leq \tfrac{1}{\beta},$$

and denoting by $|||.|||_2$ the matrix norm subordinate to the Euclidean norm, we have:

Proposition B.6. *Let A belong to $\mathcal{P}_{2^{N+1}-1}$, then*

$$|||A^{-1}|||_2 \leq (2^{N+1}-1) \max\left[\frac{\alpha}{\beta^2}\left(1+\frac{\alpha}{\beta}\right)^{N-2}, \frac{1}{\beta}\right].$$

C. Appendix: Iterative process

In Section 6, we found a fixed point of F. However, we did not prove uniqueness nor supplied a constructive method. In this part, we prove that under more restrictive hypothesis, the Picard fixed point theorem can be applied. Here, we assume that Theorem 4.15 is verified. Let us begin with the convergence and convergence speed of the iteration scheme defined by:

$$\mathbf{q}^0 \in \Omega,\ \mathbf{q}^1 = F(\mathbf{q}^0),\ \mathbf{q}^2 = F(\mathbf{q}^1), ... \tag{C.1}$$

To do so, we look for a constant $0 < C < 1$ such that

$$||F(\mathbf{q}^2) - F(\mathbf{q}^1)||_2 \leq C||\mathbf{q}^2 - \mathbf{q}^1||_2.$$

More precisely, we will prove that $\nabla_{\mathbf{q}} F$ is bounded and that its bounds can be adjusted thanks to models parameters in order to apply Picard Theorem.

First, recalling that $F = f \circ \mathbf{r}$, with f given by (5.1), from the chain rule together with $G(\mathbf{r}, \mathbf{q}) = 0$, it follows that:

$$\nabla_{\mathbf{q}} F(\mathbf{q}) = \nabla_{\mathbf{r}} f(\mathbf{r}(\mathbf{q})).\nabla_{\mathbf{q}} \mathbf{r}(\mathbf{q}) = -\nabla_{\mathbf{r}} f(\mathbf{r}(\mathbf{q})).\left[\left[\nabla_{\mathbf{r}} G(\mathbf{r}(\mathbf{q}), \mathbf{q})\right]^{-1}.\nabla_{\mathbf{q}} G(\mathbf{r}(\mathbf{q}), \mathbf{q})\right]. \tag{C.2}$$

The expression of $\nabla_{\mathbf{q}} F$ leads us to study the three gradients of the right-hand side of equation (C.2).

C.1. Gradients

In this part, we calculate the three gradients of the right-hand side of (C.2).

C.1.1. *Calculation of* $\nabla_{\mathbf{r}} G$

First, we recall that for all $i \in \{1, ..., 2^{N+1} - 1\}$:

$$\tilde{p}_i = P_{root} + \sum_{j \in \Pi_{0 \to i}} \frac{3C\tilde{r}_j^e}{\tilde{r}_j^4} \tilde{q}_j, \tag{C.3}$$

hence $(\mathbf{r}, \mathbf{q}) \to \alpha_i(\mathbf{r}, \mathbf{q})$, given by (4.16), has zero derivatives $\frac{\partial \alpha_i}{\partial r_j}(\mathbf{r}, \mathbf{q})$ if $j \notin \Pi_{0 \to i}$ or $j = i$. Furthermore, we have:

Proposition C.1. *The matrix $\nabla_{\mathbf{r}} G$ is triangular. It belongs to $GL_{2^{N+1}-1}(\mathbf{R})$ and is given by:*

$$\frac{\partial G_i}{\partial r_j}(\mathbf{r}, \mathbf{q}) = \begin{cases} \frac{\alpha_i(\mathbf{r},\mathbf{q})}{\tilde{r}_i^e} - \frac{3\eta\tilde{q}_i}{\tilde{r}_i^4} & \text{if } j = i \\ -\frac{30C\tilde{r}_j^e \tilde{r}_i}{E\tilde{r}_i^e \tilde{r}_j^5} \tilde{q}_j & \text{if } j \in \Pi_{0 \to i},\ j \neq i \\ 0 & \text{elsewhere.} \end{cases}$$

Proof. The fact that $\frac{\partial G_i}{\partial_{r_i}}(\mathbf{r}, \mathbf{q}) \neq 0$ comes from the assumption $\alpha_i(\mathbf{r}, \mathbf{q}) < 0$ together with $\tilde{q}_i \geq 0$. □

Remark C.2. The matrix $\nabla_{\mathbf{r}} G$ is a sparse matrix which has at most $\sum_{k=0}^{2^{N+1}-1} (k+1)2^k$ non vanishing terms (it has at most $(k+1)2^k$ non vanishing terms on line k). Moreover, it belongs to the set $\mathcal{P}_{2^{N+1}-1}$ studied in Appendix B.

C.1.2. *Calculation of* $\nabla_{\mathbf{q}} G$

First, recall that for all j in $\{1, ..., 2^{N+1} - 1\}$:

$$\tilde{q}_j = \sum_{k \text{ s.t. } j \in \Pi_{0 \to 2^N + k}} q_k,$$

hence:

$$\frac{\partial \tilde{q}_j}{\partial q_k} = \begin{cases} 1 & \text{if } j \in \Pi_{0 \to 2^N + k} \\ 0 & \text{else.} \end{cases}$$

Obviously, from (C.3), we deduce that:

$$\frac{\partial \tilde{p}_i}{\partial q_k}(\mathbf{r}, \mathbf{q}) = \sum_{j \in \Pi_{0 \to i}} \frac{6C\tilde{r}_j^e}{\tilde{r}_j^4} \frac{\partial \tilde{q}_j}{\partial q_k} = \sum_{j \in \Pi_{0 \to i} \cap \Pi_{0 \to k}} \frac{6C\tilde{r}_j^e}{\tilde{r}_j^4}. \tag{C.4}$$

Moreover, recalling the expression of G, we have

$$\frac{\partial G_i}{\partial q_k} = \frac{\partial \alpha_i}{\partial q_k} \frac{\tilde{r}_i}{\tilde{r}_i^e} + \frac{\eta}{\tilde{r}_i^3} \frac{\partial \tilde{q}_i}{\partial q_k},$$

hence, using the expression of α_i, we obtain

$$\frac{\partial G_i}{\partial q_k} = \frac{15C\tilde{r}_i}{E\tilde{r}_e^i} \left[\sum_{j \in \Pi_{0 \to [\frac{i}{2}]} \cap \Pi_{0 \to k}} \frac{\tilde{r}_j^e}{\tilde{r}_j^4} \right] + \frac{\eta}{\tilde{r}_i^3} \frac{\partial \tilde{q}_i}{\partial q_k}. \tag{C.5}$$

C.1.3. *Calculation of* $\nabla_{\mathbf{r}} f$

Note that f can be decomposed as $f(\mathbf{r}) = Q \circ B^N(\mathbf{r})$ with

$$Q(A) = \frac{A^{-1}J}{{}^tJA^{-1}J}\Phi \quad \text{for } A \in S_{2^N}^{+*}$$

and $B^N(\mathbf{r})$ being the matrix associated to a tree $\mathcal{T}_N$ with an $\mathbf{r}$ distribution of radii as in Proposition 4.6.

A simple calculation gives the differential of Q:

$$D_A Q(A).H = \left[\frac{{}^tJA^{-1}HA^{-1}J}{({}^tJA^{-1}J)^2} A^{-1} - \frac{A^{-1}HA^{-1}}{{}^tJA^{-1}J} \right] J\Phi. \tag{C.6}$$

The differential of the application $\mathbf{r} \to B^N(\mathbf{r})$ is easy to calculate, because every coefficient (i, j) of $B^N(\mathbf{r})$ is a sum of resistance terms $\tilde{R}_k = 6Cr_k^e/r_k^4$ with k in a subset $N_{i,j}$ of $\{1, ..., 2^{N+1} - 1\}$. $N_{i,j}$ has the property that if $k, l \in N_{i,j}$, with $k \neq l$, then $g(k) \neq g(l)$ (hence there is a maximum of N terms, reached on diagonal), see Proposition 4.6 and Definition 4.8. Then, we can write for all (i, j) in $\{1, ..., 2^{N+1} - 1\}$:

$$B^N(\mathbf{r})_{i,j} = \sum_{k \in N_{i,j}} \frac{6C\tilde{r}_k^e}{\tilde{r}_k^4}$$

and consequently:

$$\left(\nabla_r B^N(\mathbf{r}).h\right)_{i,j} = \sum_{k \in N_{i,j}} \frac{-24Cr_e^k}{r_k^5} h_k. \tag{C.7}$$

Finally, the chain rule yields:

$$\nabla_{\mathbf{r}} f(\mathbf{r}).h = D_A Q(B^N(\mathbf{r})).[\nabla_{\mathbf{r}} B^N(\mathbf{r}).h].$$

C.2. **Estimates**

In this part we give the estimates of the three gradients of the right-hand side of equation (C.2).

C.2.1. *Estimates of* $\nabla_{\mathbf{r}} G$

Recalling the definition of $\nabla_{\mathbf{r}} G$, we know that it belongs to $\mathcal{P}_{2^{N+1}-1}$, hence we can apply Proposition B.6 and we can give estimates on α and β given by (B.1). For simplicity, we will now denote $A = (a_{ij})$ the matrix $\nabla_{\mathbf{r}} G$.

Estimate of α:

We assume in this paragraph that $i \neq j$. We recall that:

$$a_{ij} = -\frac{30C\tilde{r}_j^e \tilde{r}_i}{E\tilde{r}_i^e \tilde{r}_j^5}\tilde{q}_j \qquad \text{if } j \in \text{path}_{0\to i}$$
$$a_{ij} = 0 \qquad \text{else.}$$

Hence:

$$|a_{ij}| \leq \frac{30C\tilde{r}_j^e \tilde{r}_{k(i)}^{max}}{E\tilde{r}_i^e (\tilde{r}_{g(j)}^{min})^5}\tilde{q}_{g(j)}^{max},$$

and

$$\alpha = \max_{i\in\{1,\dots,2^N-1\},\ j\in\text{path}(0\to i), j\neq i} \frac{60C\tilde{r}_j^e \tilde{r}_{k(i)}^{max}}{\tilde{r}_i^e (\tilde{r}_{g(j)}^{min})^5}\tilde{q}_{g(j)}^{max}. \tag{C.8}$$

Estimate of β:

According to the previous definition:

$$a_{ii} = \frac{\alpha_i(\mathbf{r},\mathbf{q})}{\tilde{r}_i^e} - \frac{3\eta\tilde{q}(i)}{\tilde{r}_i^4}$$

where we recall that

$$\alpha_i = -1 - \frac{5\Big((P_0 - \tilde{p}_{[\frac{i}{2}]}) + (P_{ext}^2 - P_{ext}^1)\Big)}{2E} \text{ and } \eta = \frac{15C}{2}.$$

Within our hypothesis (which are the same as Thm. 4.15) and recalling Theorem 4.15 together with Remark 4.16, for all i in $\{1,\dots,2^{N+1}-1\}$, we have

$$-a_{ii} \geq -\frac{\alpha_{k(i)}^{max}}{\tilde{r}_i^e} + \frac{3\eta\tilde{q}_{k(i)}^{min}}{\left(\tilde{r}_{k(i)}^{max}\right)^4}.$$

According to the data of our model, the right-hand side of the previous inequality is always strictly positive, hence we can conclude that:

$$\beta = \min_{i\in\{1,\dots,2^N-1\}} -\frac{\alpha_{k(i)}^{max}}{\tilde{r}_i^e} + \frac{3\eta\tilde{q}_{k(i)}^{min}}{\left(\tilde{r}_{k(i)}^{max}\right)^4} > 0. \tag{C.9}$$

Then, along with Proposition B.6, this yields that

$$|||(\nabla_r G(\mathbf{r},\mathbf{q}))^{-1}|||_2 \leq 2^N \max\left[\frac{\alpha}{\beta^2}\left(1+\frac{\alpha}{\beta}\right)^{N-2}, \frac{1}{\beta}\right],$$

with α and β given by (C.8) and (C.9).

C.2.2. *Estimate of* $\nabla_{\mathbf{q}} G$

From equation (C.5), for all i in $\{1, ..., 2^{N+1} - 1\}$ and $k \in \{0, ..., 2^{N-1}\}$, it follows that:

$$\left|\frac{\partial G_i}{\partial q_k}\right| \leq \frac{15C\tilde{r}^{max}_{k(i)}}{E\tilde{r}^i_e}\left[\sum_{j\in\Pi(0\to[\frac{i}{2}])\cap\Pi(0\to k)} \frac{\tilde{r}^e_j}{\left(\tilde{r}^{min}_{g(j)}\right)^4}\right] + \frac{\eta}{\left(\tilde{r}^{max}_{k(i)}\right)^3} = M_{i,k}.$$

Next, we know that:

$$|||\nabla_q G(q)|||_2 \leq 2^N(2^{N+1}-1) \max_{(i,k)\in\{1,...,2^{N+1}-1\}\times\{0,...,2^{N-1}\}} \left|\frac{\partial G_i}{\partial q_k}\right|,$$

hence,

$$|||\nabla_q G(q)|||_2 \leq 2^N(2^{N+1}-1) \max_{(i,k)\in\{1,...,2^{N+1}-1\}\times\{0,...,2^{N-1}\}} M_{i,k}.$$

C.2.3. *Estimate of* $\nabla_r f$

Let us note $A = B^N(\mathbf{r})$ and let $sp(A)$ be the set of the eigenvalues of A. Here, we will use the spectral properties of the matrix A. From Proposition A.1 together with the trace and $|||.|||_2$ properties we know that:

$$\begin{aligned}
\text{If } \lambda \quad &\in \quad sp(A) \text{ then } \lambda \geq \min_{i|k(i)=N} \tilde{R}_i. && \text{(C.10)}\\
\lambda_{min} \quad &= \quad \min(sp(A)) \text{ verifies } \lambda_{min} \leq tr(A)/2^N. && \text{(C.11)}\\
\lambda_{max} \quad &= \quad \max(sp(A)) \text{ verifies } tr(A)/2^N \leq \lambda_{max} \leq tr(A). && \text{(C.12)}\\
|||A^{-1}|||_2 \quad &= \quad 1/\lambda_{min}. && \text{(C.13)}\\
||J||_2^2 \quad &= \quad 2^N. && \text{(C.14)}
\end{aligned}$$

According to the formula of $\nabla_r f$ given in Section C.1.3, we need to estimate the following terms ${}^tJA^{-1}J$, $D_AQ(A).H$ and A^{-1} with correct norms.

Estimate of ${}^tJA^{-1}J$**:**

Since A^{-1} is a symmetric positive definite matrix (because A is, see Prop. A.1), we know that it is coercive and that its coercive constant is its smallest eigenvalue, *i.e.*:

$${}^tJA^{-1}J \geq \min_{\lambda\in sp(A)}\left(\frac{1}{\lambda}\right) \times ||J||_2^2 = \frac{||J||_2^2}{\lambda_{max}}.$$

Moreover,

$$tr(A) = \sum_{j=1}^{2^{N+1}-1} 2^{N-g(j)}\tilde{R}_j,$$

and recalling that $\tilde{R}_j \leq \frac{6Cr^e_j}{(r^{min}_{g(j)})^4}$, we have:

$$tr(A) \leq 6C\sum_{k=1}^{N}\left(\frac{2^{N-k}}{(\tilde{r}^{min}_k)^4}\sum_{j\ st\ g(j)=k} r^e_j\right).$$

Let us call $m_1(\mathcal{T}_N)$ the right-hand side term of the previous inequality divided by 2^N, then $tr(A) \leq 2^N m_1(\mathcal{T}_N)$, where $m_1(\mathcal{T}_N)$ only depends on the parameters of the model (which are the unconstrained radius, the pressures P_{ext}, the root pressure, P_0, E and Φ). Then, using (C.12), we obtain:

$$ {}^tJA^{-1}J \geq \frac{1}{tr(A)}||J||_2^2 \geq \frac{2^N}{2^N m_1(\mathcal{T}_N)} \geq m_1(\mathcal{T}_N)^{-1}. \tag{C.15}$$

Estimate of $D_AQ(A).H$:

Thanks to the previous inequality, and from Section C.1.3 we have:

$$|||D_AQ(A).H|||_2 \leq \Big(2^N m_1(\mathcal{T}_N)|||A^{-1}|||_2^3 + |||A^{-1}|||_2^2\Big) m_1(\mathcal{T}_N)\Phi 2^{N/2}||H||_2. \tag{C.16}$$

Next, taking $H = \nabla_r A.h$ in (C.16), and recalling equation (C.7) we obtain an upper bound:

$$||\nabla_r A.h||_2 \leq 2^N \max_{i,j\in\{1,\dots,2^N\}} |a_{ij}| \leq 2^N 24c||r_e||_\infty ||h||_2 \sum_{g=1}^{N} \left(\frac{1}{\tilde{r}_g^{min}}\right)^5.$$

Let us set $m_2(\mathcal{T}_N) = 2^N 24c||r_e||_\infty \sum_{g=1}^N 1/(\tilde{r}_g^{min})^5$, which only depends on the parameters of the model. We have:

$$||\nabla_r A.h||_2 \leq m_2(\mathcal{T}_N)||h||_2.$$

Estimate of A^{-1}:

Using (C.10) and (C.13), we deduce that

$$|||A^{-1}|||_2 \leq \frac{1}{\min_{i|k(i)=N} \tilde{R}_i} \leq \frac{(\tilde{r}_N^{max})^4}{6c \min_{i|k(i)=N}(r_e^i)} = m_3(\mathcal{T}_N), \tag{C.17}$$

and $m_3(\mathcal{T}_N)$ only depends on the parameters of the model.

Estimate of $\nabla_r f$:

Using previous estimates (C.15)–(C.17), we deduce that:

$$\begin{aligned} |||\nabla_r f(r).h|||_2 &= |||D_AQ(\nabla_r A.h)|||_2 \\ &\leq 2^{\frac{N}{2}}\Big(2^N m_1(\mathcal{T}_N)m_3(\mathcal{T}_N) + 1\Big) m_1(\mathcal{T}_N)^2 m_2(\mathcal{T}_N) m_3(\mathcal{T}_N)^2 \Phi ||h||_2. \end{aligned} \tag{C.18}$$

C.2.4. *Final estimate*

Combining all results (C.15)–(C.18) from this section allows us to get an upper bound of $|||\nabla_q F(q)|||_2$:

$$\nabla_{\mathbf{q}} F(\mathbf{q}).h = -\nabla_{\mathbf{r}} f(\mathbf{r}(\mathbf{q})).\left[\left[\nabla_{\mathbf{r}} G(\mathbf{r}(\mathbf{q}),\mathbf{q})\right]^{-1}.\nabla_{\mathbf{q}} G(\mathbf{r}(\mathbf{q}),\mathbf{q}).h\right].$$

Hence there exists a constant $C(\mathcal{T}_N,\Phi)$ such that for all $h \in \mathbf{R}^{2^N}$, $||\nabla_{\mathbf{q}} F(\mathbf{q}).h||_2 \leq C(\mathcal{T}_N,\Phi)\Phi||h||_2$, therefore:

$$|||\nabla_{\mathbf{q}} F(\mathbf{q})|||_2 \leq C(\mathcal{T}_N,\Phi)\Phi.$$

This leads to the proof of the Theorem 6.5, recalled below:

Theorem C.3. */ 6.5 There exists $\eta > 0$ such that if Φ belongs to $[0,\eta[$ then the Picard fixed-point theorem applies for F on $\Omega_{\epsilon_{\mathcal{T}_N}}$. This leads to uniqueness of the fixed point $\mathbf{q}_F$ of F in $\Omega_{\epsilon_{\mathcal{T}_N}}$ and to convergence of Proposition C.1 toward $\mathbf{q}_F$.*

Proof. We just need to prove that if Ψ is a strictly positive real number, then for all Φ in $[0, \Psi]$, there exists $K(\mathcal{T}_N) > 0$ such that

$$C(\mathcal{T}_N, \Phi) \leq K(\mathcal{T}_N).$$

This property is a consequence of the fact that $q_j^{min} \geq 0$ and $q_j^{max} \leq \Psi$ for all Φ in $[0, \Psi]$ and that the estimates from this chapter can be obtain in a similar way but independently of Φ, with $q_j^{min} = 0$ and $q_j^{max} = \Psi$. □

Remark C.4. In the same way, it can be shown there exists $E_{min} > 0$ such that if $E > E_{min}$ then the Picard Theorem applies on F.

Remark C.5. The Theorem C.3 and the Remark C.4 prove that the Picard Theorem better applies for small deformations, which is consistent with the linear elasticity model used for bronchial wall deformation.

Acknowledgements. The authors wish to thank Professors Le Dret and Maury for very helpful discussions and the CMLA (ENS de Cachan, France) for access to Matlab 7.

References

[1] P. Dejours, *Principles of Comparative Respiratory Physiology*. Elsevier/North-Holland Biomedical Press (1982).
[2] P. Feynman, *Electromagnétisme 2*. InterEditions (1979).
[3] C. Grandmont, B. Maury and N. Meunier, A viscoelastic model with non-local damping application to the human lungs. *ESAIM: M2AN* **40** (2006) 201–224.
[4] B. Housset, *Pneumologie*. Masson (1999).
[5] B. Mauroy, *Hydrodynamique dans le poumon, relations entre flux et géométries*. Ph.D. thesis, ENS de Cachan (2004), http://www.cmla.ens-cachan.fr/∼mauroy/mauroy_these.pdf
[6] B. Mauroy, M. Filoche, J.S. Andrade, Jr., and B. Sapoval, Interplay between geometry and flow distribution in an airway tree. *Phys. Rev. Lett.* **90** (2003) 148101.
[7] B. Mauroy, M. Filoche, E.R. Weibel and B. Sapoval, An optimal bronchial tree may be dangerous. *Nature* **427** (2004) 633–636.
[8] B. Maury and C. Vannier, *Une modélisation du poumon humain par un arbre infini*. CANUM (2006).
[9] M.L. Oelze, R.J. Miller and J.P. Blue, Jr., Impedance measurements of ex vivo rat lung at different volumes of inflation. *J. Acoust. Soc. Am.* **114** (2003) 3384–3393.
[10] F. Preteux, C. Fetita, A. Capderou and P. Grenier, Modeling, segmentation, and caliber estimation of bronchi in high-resolution computerized tomography. *J. Electron. Imaging* **8** (1999) 36–45.
[11] F.G. Salerno and M.S. Ludwig, Elastic moduli of excised constricted rat lungs. *J. Appl. Physiol.* **86** (1999) 66–70.
[12] E.R. Weibel, *Morphometry of the Human Lung*. Springer, Verlag (1963).
[13] E.R. Weibel, *The Pathway for Oxygen*. Harvard University Press (1984).
[14] G.B. West, J.H. Brown and B.J. Enquist, A general model for the origin of allometric scaling laws in biology. *Science* **276** (1997) 122–126.
[15] M.S. Zach, The physiology of forced expiration. *Paed. Resp. Review* **1** (2000) 36–39.